# Self-Assembled Highly Positively Charged Allyl-Pd Crowns: Cavity-Pocket Driven Interactions of Fluoroanions.

Montserrat Ferrer,[a,*] Albert Gallen,[a] Albert Gutiérrez,[a] Manuel Martínez,[a] Eliseo Ruiz,[a, b] Yvonne Lorenz[c] and Marianne Engeser[c]

[a] *Departament de Química Inorgànica i Orgànica, Secció de Química Inorgànica. Universitat de Barcelona, c/ Martí i Franquès 1-11 08028 Barcelona, Spain.*

[b] *Institut de Química Teòrica i Computacional, Universitat de Barcelona, c/ Martí i Franquès 1-11, 08028 Barcelona, Spain*

[c] *Kekulé-Institute for Organic Chemistry and Biochemistry, University of Bonn, Gerhard-Domagk-Str. 1, 53121 Bonn, Germany*

**Abstract**

A series of dodecanuclear highly positively charged homo- and heterometallamacrocycles $[\{Pd(\eta^3\text{-}2\text{-}Me\text{-}C_3H_4)\}_6(4\text{-}PPh_2py)_{12}\{M_2(tpbz)\}_3]^{18+}$ (M = Pd, Pt; tpbz = 1,2,4,5-tetrakis(diphenylphosphanylbenzene) were synthesized by the quantitative self-assembly of $\{Pd(\eta^3\text{-}2\text{-}Me\text{-}C_3H_4)\}^+$, $\{M_2(tpbz)\}^{4+}$ and $4\text{-}PPh_2py$ moieties in 2:1:4 molar ratio. The cationic assemblies were obtained as salts of different fluorinated anions that display diverse sizes and electronic properties, namely $BF_4^-$, $PF_6^-$, $SbF_6^-$ and $CF_3SO_3^-$. The new crown-like metallamacrocycles showed remarkable differences in their NMR spectra due to the presence of the different counteranions. On the basis of the observed variations, the metallacycles have been tested as catalytic precursors in allylic alkylation reactions. The anion-dependent activity and selectivity has been analysed and compared with that of the corresponding monometallic allylic corners $[Pd(\eta^3\text{-}2\text{-}Me\text{-}C_3H_4)(4\text{-}PPh_2py)_2]X$ (X = $BF_4^-$, $PF_6^-$, $SbF_6^-$, $CF_3SO_3^-$). DFT calculations have been employed in order to help to the interpretation of the experimental data and to model the anion-crown interactions.

## Introduction

Coordination-driven assembly of organic ligands and metal ions plays a key role in the construction of nanoscale molecular well-defined architectures.[1] Particularly,

supramolecular metallamacrocycles self-assembled from many components often bear specific functionalities, conferring them unique properties that account for their potential applications. The properties of these macro assemblies can be modulated by the rational choice of both the specific functionalities in the constituent organic frameworks and the metal ions. In this way, the constructed supramolecules can be involved in host–guest chemistry,[2] or present photophysical,[3] redox[4] and/or catalytic activity,[5] among others features.[6]

Apart from the directing elements imposed by the building blocks, the outcome of the self-assembly reactions is also controlled by other factors such as reagents concentration, solvent, or counteranions. The ability of anions to operate as templates (or guests) and have a significant influence on the course of the assembly process through noncovalent interactions is well documented.[7] Furthermore, the establishment of this kind of weak interactions can exert a subtle control of the catalyst behaviour that could depend on the nature of the counteranion.[8]

We recently reported the self-assembly of a series of tetranuclear homo- and heterometallamacrocycles that incorporate the allyl-palladium function $\{Pd(\eta^3\text{-}2\text{-}Me\text{-}C_3H_4)\}^+$.[9] Since this organometallic fragment is well known for its relevance as precursor of the catalytically active species in several metal-catalysed organic transformations,[10] we studied the allylic alkylation of the 3-acetoxy-phenyl-1-propene catalysed by the polymetallic architectures $[\{Pd(\eta^3\text{-}2\text{-}Me\text{-}C_3H_4)(4\text{-}PPh_2py)_2\}_2\{M(dppp)\}_2](CF_3SO_3)_6$ (M=Pd, Pt) (dppp= 1,3-bis(diphenylphosphino)propane) in comparison with that of the corresponding active monometallic complex $[Pd(\eta^3\text{-}2\text{-}Me\text{-}C_3H_4)(4\text{-}PPh_2py)_2](CF_3SO_3)$. In spite of the crowded environment around the active catalytic fragment in the supramolecular species, we did not observe significant differences on the regioselectivity of the metallamacrocycles compared with that of the unassembled catalytically active precursor.

These disappointing results lead us to investigate the effect of the increase of the nuclearity and hence the size of the metallacycles in order to induce a change in the environment of the allyl-palladium moiety that could definitively modify the catalytic outcome of the supramolecular compound. We considered thus the use of a bis(chelating)tetraphosphane as a spacer, which should give rise to the formation of two equivalent square-planar entities connected by a phenyl ring. In this respect, even though extensive research has been conducted over the past decades, examples of

supramolecular metallamacrocycles containing polyphosphane ligands as linkers are relatively scarce. Due to the free rotation around the P–C bond, different orientations of the lone pair of electrons of the phosphanes are possible, resulting in a poor predictability of the assembled species.[11] Hence, in order to force a pre-designed self-assembly, steric constraints have to be introduced into the polyphosphane backbone. In general, then, the cage compounds that are held together by polyphosphanes contain rigid benzene[12] or benzene-like units.[13]

With all these considerations in mind, we succeeded in obtaining in a selective way a set of highly charged dodecametallic crown-like $[\{M(\eta^3\text{-2-Me-}C_3H_4)\}_6(4\text{-}PPh_2py)_{12}M'_6(tpbz)_3]^{+18}$ (M = Pd, M'= Pd, Pt) architectures by means of a three-component self-assembly process between the $Pd^{II}$ or $Pt^{II}$ derivatives of the tetratopic 1,2,4,5-tetrakis(diphenylphosphino)benzene (tpbz), $\{Pd(\eta^3\text{-2-Me-}C_3H_4)\}^+$ and the ambidentate 4-$PPh_2$py ligand, specifically designed[9a, 14] to induce a favoured coordination to the metal centres according to the antisymbiotic effect.

Given the high positive charge of the obtained polymetallic species, and the concomitant presence of an important number of anions as charge-balance components, we have synthesized a series of derivatives with different fluoroanions *i. e.* $BF_4^-$, $PF_6^-$, $SbF_6^-$ and $CF_3SO_3^-$ and studied its behaviour in solution by multinuclear NMR spectroscopy. The obtained results strongly confirmed the keystone influence of the counteranions on the self-assembly process. Although this effect is usually associated with the coordinating ability of the anions,[15] other factors including, the size,[16] shape,[17] or even the solubility of the corresponding salt in a specific solvent can not be ruled out. Finally, as indicated above, the activity of the assemblies as homogeneous catalysts in the allylic alkylation process has been undertaken.

## Results and discussion

With the aim of preparing allyl-Pd metallamacrocycles having higher nuclearities than those reported before by our group,[9a, 14] the previous synthesis and full characterization of the required building blocks was carried out.

### Synthesis and Characterization of 1,2,4,5-tetrakis(diphenylphosphino)benzene (tpbz) bimetallic building blocks.

The bimetallic compounds $[M_2(tpbz)(solvent)_4]X_4$ (M = Pd; X = $BF_4^-$, **2Pd**, $PF_6^-$, **3Pd**, $SbF_6^-$, **4Pd;** M = Pt; X = $BF_4^-$, **2Pt**, $PF_6^-$, **3Pt**, $SbF_6^-$, **4Pt**, $PF_2O_2^-$, **5Pt**) were synthesized following a modified procedure from that described for the $CF_3SO_3^-$ derivatives by Dalcanale et al.[18] The reaction of the silver salt of the chosen anion with $[M_2(tpbz)Cl_4]$ in 4:1 molar ratio in a dichloromethane/acetonitrile mixture (1:1 in volume) at RT for 12 h resulted in a suspension that after filtration, concentration and precipitation upon addition of dimethylether afforded the desired compounds as a solvato complexes. While four molecules of either acetonitrile (**2Pd-3Pd**) or water (**4Pd**) are coordinated to the $Pd^{II}$ centre, in the case of the $Pt^{II}$ species (**2Pt-4Pt**) the complex second order $^{31}P$ NMR spectra (Figures S12, S16 and S21) are indicative of the coexistence of two molecules of both acetonitrile and water in the coordination sphere of the metallic cation. Only for the $PF_2O_2^-$ derivative the anions appear coordinated to the $Pt^{II}$ centre, producing a much more insoluble compound. All attempts to obtain the analogous $BArF^-$ (tetrakis[3,5-bis(trifluoromethyl)phenyl]borate) derivatives were unsuccessful.

**Synthesis and Characterization of $[Pd(\eta^3\text{-}2\text{-}Me\text{-}C_3H_4)(4\text{-}PPh_2py)]X$ (X = $BF_4^-$ (2a), $PF_6^-$ (3a), $SbF_6^-$ (4a), $BArF^-$ (5a)) ditopic building blocks.**

Although the obtention of our crown-like metallamacrocycles was effective by a three-component self-assembly, an alternative synthetic pathway that only involves two building blocks provided comparable results (Scheme 1). For this purpose, the preliminary synthesis of the allyl palladium donor $[Pd(\eta^3\text{-}2\text{-}Me\text{-}C_3H_4)(4\text{-}PPh_2py)_2]^-$ with the studied anions was conducted. As described in the literature for the triflate derivative,[9a] the addition of 4-$PPh_2$py to a dichloromethane solution of the suitable $[Pd(\eta^3\text{-}2\text{-}Me\text{-}C_3H_4)(cod)]X$ (X = $BF_4^-$, $PF_6^-$, $SbF_6^-$, $BArF^-$) in 2:1 molar ratio gave the desired products (**2a-5a**) in good yields. Distinctive variations in the allyl region of the $^1H$ NMR of the mononuclear complexes as a function of the counteranion were observed (Figure S51 and Table S1 in Supporting Information). Although in the case of $BF_4^-$, $PF_6^-$, $CF_3SO_3^-$ and $BArF^-$ derivatives two singlets due to the *syn* and *anti* protons of the allyl ligand respectively, are observed, only one broad signal of intermediate chemical shift is obtained for the $SbF_6^-$ species. In this respect, the noticeable progressive decrease ($BArF^- > CF_3SO_3^- > BF_4^- > PF_6^-$) in the $\delta_{syn} - \delta_{anti}$ value indicates an increase of the dynamic exchange rate of the allyl ligand depending on the counteranion. The observed trend concerning fluxionality rates does not agree with the

coordinating ability of the different fluoroanions utilised, thus suggesting the prevalence of weak interactions involving the terminal fluoro atoms and the allyl-Pd building block.[8] Clearly, this differential behaviour could have a decisive influence on the self-assembly process of the metallamacrocycles, as described below.

**Self-Assembly of [{Pd($\eta^3$-2-Me-$C_3H_4$)}$_6$(4-$PPh_2$py)$_{12}${$M_2$(tpbz)}$_3$]$X_{18}$ dodecanuclear crown-like metallamacrocycles.**

Having in mind our design strategy, we proceeded with the combination of the triflate salts of $[M_2(tpbz)(solvent)_4]^{4+}$ (M = Pd, Pt) and $\{Pd(\eta^3\text{-2-Me-}C_3H_4)\}^+$ and the 4-$PPh_2$py ligand in a 1:2:4 molar ratio. In principle, the attempted self-assembly might be compatible with the formation of different cyclic assemblies i. e. [3+6+12], [4+8+16] or even higher nuclearity systems that could be polymeric. Moreover, due to both the large number of assembled units and/or their flexibility, the obtention of an equilibrium mixture among different possible architectures could not be ruled out.

The $^{31}P\{^1H\}$ NMR spectra (Figures S26 for M = Pd and S29 for M = Pt) of the solutions obtained after stirring in $CH_2Cl_2$ a mixture of the above indicated species for 2 hours at room temperature, showed a singlet associated with the P atom of the 4-$PPh_2$py unit (25.6 ppm for the Pd derivative **1a$_6$1Pd$_3$** and 26.0 ppm for the Pt derivative **1a$_6$1Pt$_3$**) and another of the tpbz ligand (55.2 ppm for **1a$_6$1Pd$_3$** and 29.1 ppm for **1a$_6$1Pt$_3$**: the latter flanked with the expected $^{195}$Pt satellites $^2J(^{31}P\text{-}^{195}Pt)$ = 3245 Hz). Thus, despite the possibility of formation of several cages, the assembly of a single discrete, highly symmetric species is exclusively observed. Identical results were obtained when the preformed donor moiety [Pd($\eta^3$-2-Me-$C_3H_4$)(4-$PPh_2$py)$_2$]$CF_3SO_3$ was treated with either the palladium or the platinum acceptor $[M_2(tpbz)(solvent)_4](CF_3SO_3)_4$ (M = Pd, Pt) in 2:1 molar ratio under the same conditions (Scheme 1). Concentration of the resulting solutions and addition of diethyl ether lead to the isolation of the metallasupramolecular species as pale yellow solids in good yields.

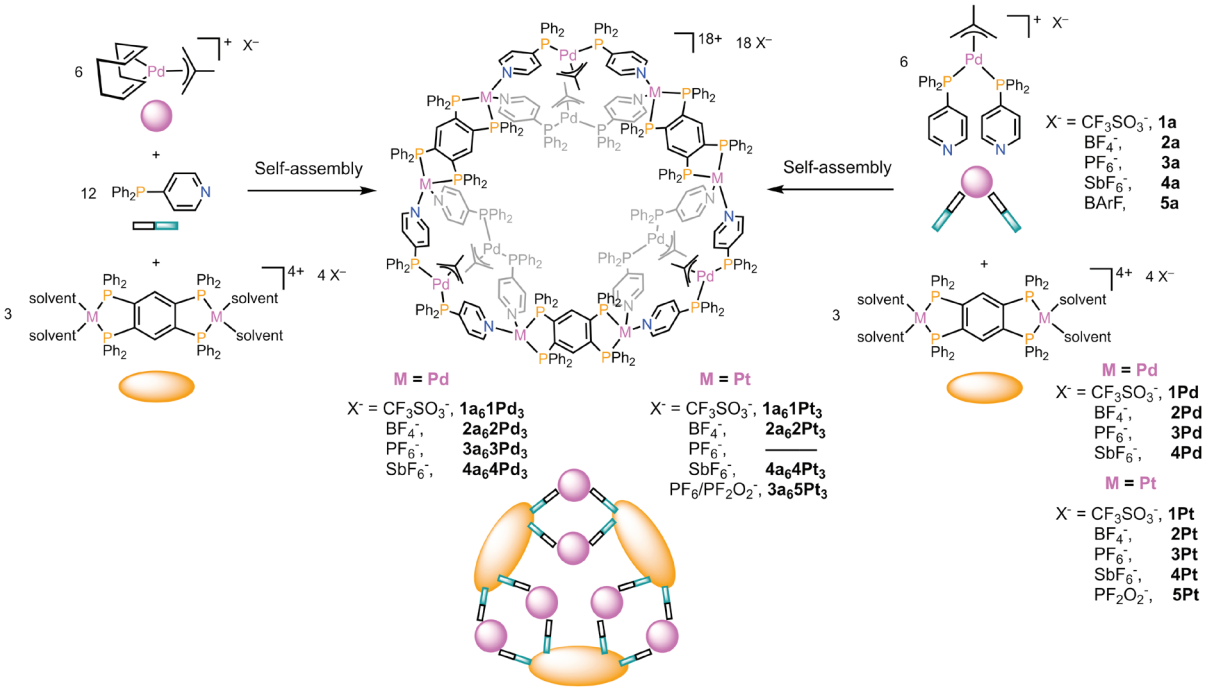


**Scheme 1**. Self-assembly pathways for the formation of the different crown-like metallamacrocycles.

The formation of a single product was further confirmed using $^{1}$H DOSY NMR, which gives a single set of peaks (Figure 1) with a diffusion coefficient of 4.3 10 $^{-10}$ m$^{2}$ s$^{-1}$ from which a hydrodynamic radius of 1.5 nm can be estimated using the Stokes-Einstein relationship, which is consistent with the crystal structure data (see below).

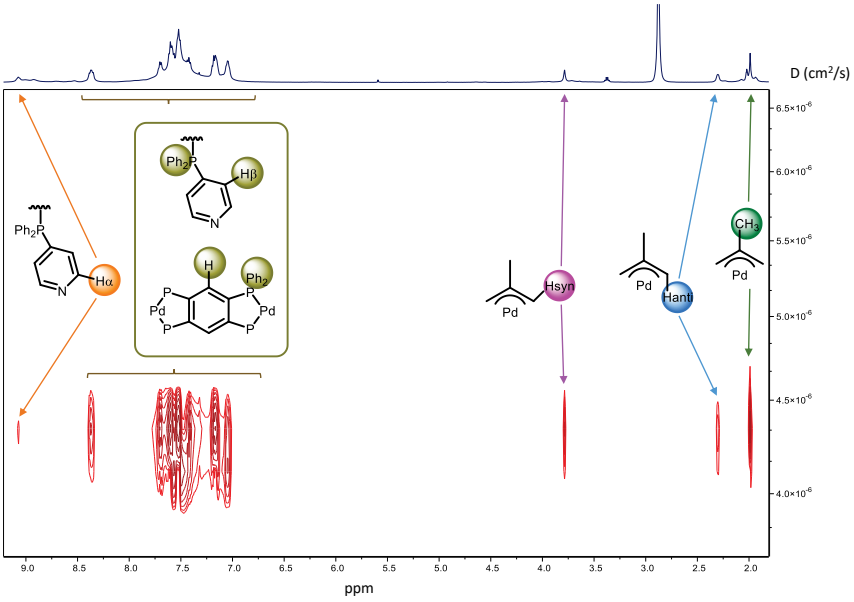

**Figure 1**. $^{1}$H DOSY NMR spectrum of [{Pd($\eta^3$-2-Me-$C_3H_4$)}$_6$(4-$PPh_2py$)$_{12}${$Pd_2$(tpbz)}$_3$]($CF_3SO_3$)$_{18}$ (**1a$_6$1Pd$_3$**) in acetone-$d_6$ at 298 K.

The exact nuclearity of the assemblies was determined unambiguously by High Resolution ESI Mass Spectrometry. The presence of signals at *m/z* = 2324.55, 1830.80 and 1499.88, corresponding to [**1a$_6$1Pd$_3$**-4$CF_3SO_3$]$^{4+}$, [**1a$_6$1Pd$_3$**-5$CF_3SO_3$]$^{5+}$ and [**1a$_6$1Pd$_3$**-6$CF_3SO_3$]$^{6+}$ ions, respectively in the case of the Pd metallacycle (Figure 2) and at 1936.12, [**1a$_6$1Pt$_3$**-5$CF_3SO_3$]$^{5+}$; 1588.61 [**1a$_6$1Pt$_3$**-6$CF_3SO_3$]$^{6+}$; 1340.37 [**1a$_6$1Pt$_3$**-7$CF_3SO_3$]$^{7+}$ for the heterometallic PdPt derivative (Figure S30) are in agreement with the formation of [3+6+12] [$M_2$(tpbz)]$^{4+}$:{Pd($\eta^3$-2-Me-$C_3H_4$)}$^+$:4-$PPh_2py$ species. Experimental isotopic patterns centred on these *m/z* values suitably correlated with the theoretical isotopic distributions calculated for the detected ions (Figures 2 and S30).

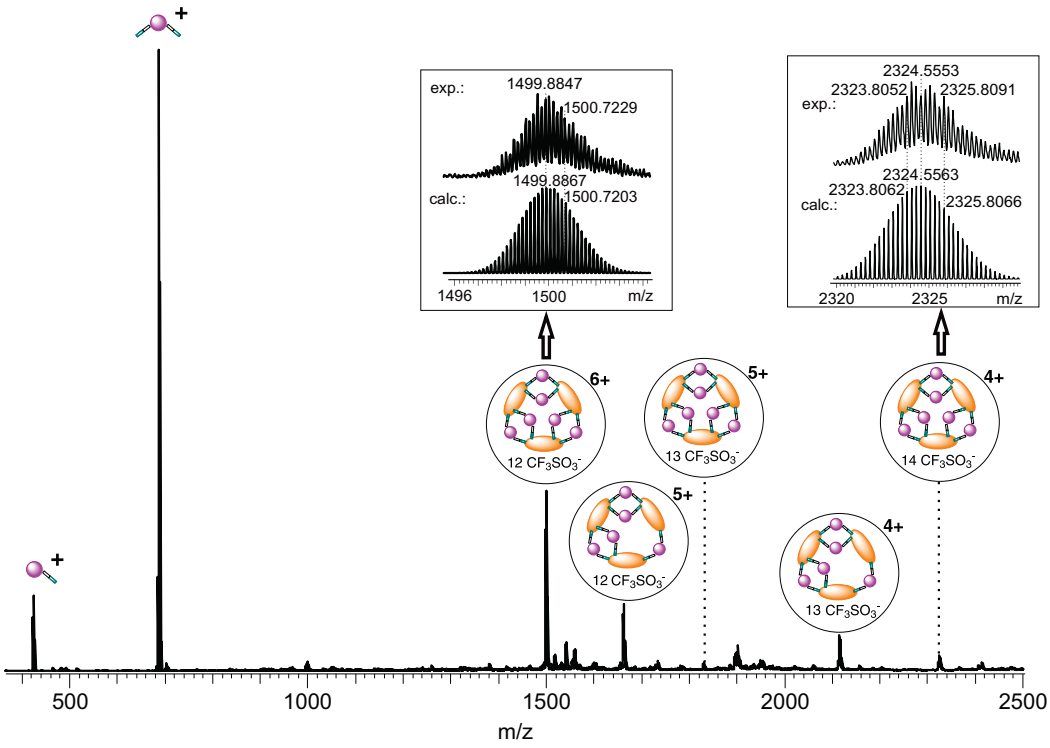


**Figure 2.** ESI(+)-HRMS spectrum of the metallamacrocycle [{Pd($\eta^3$-2-Me-$C_3H_4$)}$_6$(4-$PPh_2py$)$_{12}${$Pd_2$(tpbz)}$_3$]($CF_3SO_3$)$_{18}$ (**1a$_6$1Pd$_3$**). The insets show the concordance between the measured and calculated isotope patterns of the prominent signals [**1a$_6$1Pd$_3$**-4$CF_3SO_3$]$^{4+}$ and [**1a$_6$1Pd$_3$**-6$CF_3SO_3$]$^{6+}$.

At this point, the scope of our investigations was subsequently expanded to the study of the self-assembly reactions in the presence of other anions with different size, shape or

coordination characteristics such as $BF_4^-$, $PF_6^-$, $SbF_6^-$ and $BArF^-$. While $BF_4^-$ and $SbF_6^-$ display a coordinating ability intermediate between $CF_3SO_3^-$ and $PF_6^-$, $BArF^-$ is a very weakly coordinating species;[19] moreover, the size of $PF_6^-$ is intermediate between the large $SbF_6^-$, $BArF^-$ and $CF_3SO_3^-$ and the small $BF_4^-$. Obvious differences in shape among the used anions could also be taken into account.

All the self-assembly reactions with participation of $BF_4^-$ and $SbF_6^-$ building blocks converged into a single species in a similar way than the observed for the $CF_3SO_3^-$ compounds. Characterization data (see an exhaustive set of $^1H$, $^{31}P$, $^{19}F$ NMR and High-Resolution ESI Mass Spectrometry spectra in Supporting Information)[20] are in agreement with the exclusive formation of [3+6+12] $[M_2(tpbz)]^{4+}$:{Pd($\eta^3$-2-Me-$C_3H_4$)}$^+$:4-$PPh_2$py (M = Pd, Pt) architectures. As for the self-assembly reaction of the suitable hexafluorophosphate building blocks only the targeted Pd metallacycle [{Pd($\eta^3$-2-Me-$C_3H_4$)}$_6$(4-$PPh_2$py)$_{12}${$Pd_2$(tpbz)}$_3$]$(PF_6)_{18}$ (**3a$_6$3Pd$_3$**) was obtained. Unexpectedly, however, the presence of the $PF_2O_2^-$ anion was observed in the case of the heterometallic "**3a$_6$3Pt$_3$**" derivative most probably due to the $PF_6^-$ hydrolysis by adventitious moisture during some stage of the process. The hydrolysis of $PF_6^-$ is a common feature in coordination chemistry,[21] and it is known to occur even in $AgPF_6$, which we used to prepare [$Pd_2$(tpbz)(solvent)$_4$]$(PF_6)_4$ (**3Pd**) and [$Pt_2$(tpbz)(solvent)$_4$]$(PF_6)_4$ (**3Pt**) derivatives. A careful analysis of the assembled units revealed that $PF_6^-$ had undergone an accidental hydrolysis during the formation of the tpbz derivative and that [$Pt_2$(tpbz)$(PF_2O_2)_4$](**5Pt**) had been the actual building block instead of **3Pt**, thus allowing the formation of **3a$_6$5Pt$_3$**.

Unexpectedly, the self-assembly of [$Pt_2$(tpbz)(solvent)$_4$]$(PF_6)_4$ (**3Pt**) (obtained by reaction between [$Pt_2Cl_4$(tpbz)] and $AgPF_6$ under strictly dry conditions), [Pd($\eta^3$-2-Me-$C_3H_4$)(COD)]$PF_6$ (**3a**) and 4-$PPh_2$py did not give the expected heterometallic macrocycle "**3a$_6$3Pt$_3$**" in spite of numerous attempts. In the case of $BArF^-$ analogues, the failure of the preparation of the $[M_2(tpbz)(solvent)_4](BArF)_4$ acceptor building blocks precluded the formation of the metallamacrocycles even though several alternative strategies were attempted.

All these experiments represent a further evidence of the influence of the counteranions on self-assembly processes in a similar way to that reported by some authors in the literature for other self-assembled architectures. In particular, the presence of certain

anions like $BF_4^-$[22] or $CF_3SO_3^-$[16a] has been shown to preclude the self-assembly process giving rise to the formation of oligomers instead.

Unfortunately, most attempts to obtain single crystals for X-ray characterization of the new compounds proved to be unsuccessful. Surprisingly, we only managed to grow suitable crystals for the $[\{Pd(\eta^3\text{-}2\text{-}Me\text{-}C_3H_4)\}_6(4\text{-}PPh_2py)_{12}\{Pt_2(tpbz)\}_3](PF_6)_6(PF_2O_2)_{12}$ metallamacrocyle (**$3a_6$5$Pt_3$**), obtained by accidental hydrolysis of the $PF_6^-$ of the tpbz building block, as indicated above.

**X-Ray Crystallography**

Crystals of $[\{Pd(\eta^3\text{-}2\text{-}Me\text{-}C_3H_4)\}_6(4\text{-}PPh_2py)_{12}\{Pt_2(tpbz)\}_3](PF_6)_6(PF_2O_2)_{12}$ (**$3a_6$5$Pt_3$**) were grown by slow diffusion of diethyl ether in a dichloromethane solution of the complex at room temperature. Despite the easy efflorescence of the crystals and severe disorder of solvent molecules, the quality of X-ray structural data (Table S2 in Supporting Information) is sufficient to establish the connectivity of the structure.

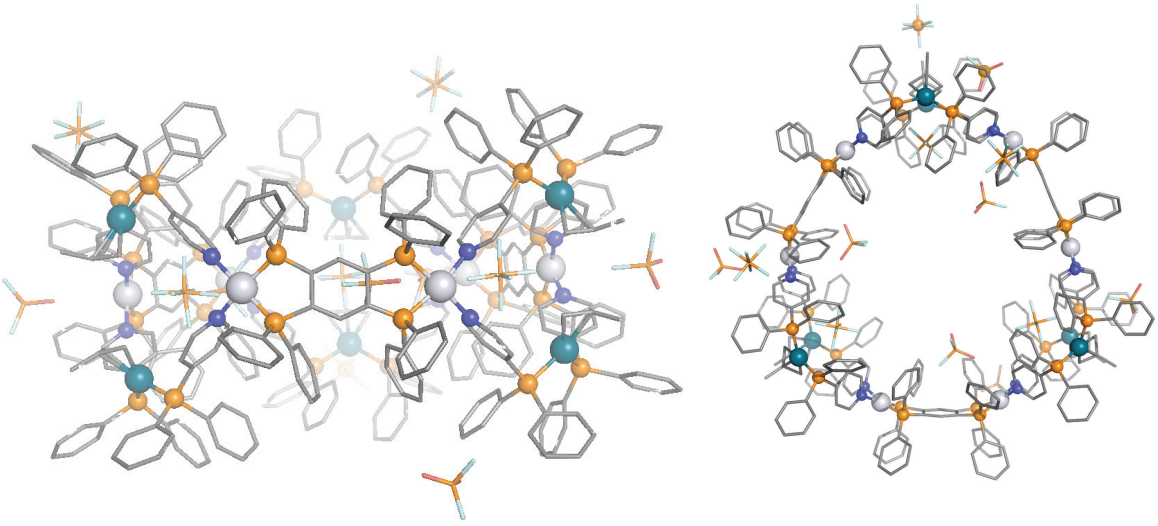

**Figure 3.** Two representations of the molecular structure obtained by X-ray diffraction of the $[\{Pd(\eta^3\text{-}2\text{-}Me\text{-}C_3H_4)\}_6(4\text{-}PPh_2py)_{12}\{Pt_2(tpbz)\}_3](PF_6)_6(PF_2O_2)_{12}$ metallamacrocycle.

The discrete crown-like structure (Figure 3) consists of three tetranuclear $Pt_2Pd_2$ butterfly shaped moieties, similar to that closely related tetranuclear metallamacrocycles recently reported by us, connected between each other by the tetraphosphane (tpbz). The $Pt^{II}$ centres are in a square planar environment determined by two phosphorus atoms of the bridging tpbz and to two pyridyl nitrogen atoms of the 4-$PPh_2$py ligands. A distorted

square planar configuration around the Pd atoms is achieved by the coordination of one allyl ligand in a $\eta^3$-fashion and two phosphorus atoms of the ditopic 4-$PPh_2py$ ligands. The distance between the farthest atoms in the metallamacrocycle is approximately 30 Å, which is in agreement with the calculated value of hydrodynamic radius from DOSY NMR experiments (15 Å). The disorder due to the high number of counteranions and the consequent limited quality of crystallographic data implies that the location of some of the anions could not be determined. However, as can be seen in Figures 3 and S53 three $PF_6^-$ and three $PF_2O_2^-$ are located in the cylindrical cavity whose dimension can be estimated to be $r_{base} \approx 10$ Å and $h \approx 9$ Å.

**$^1$H NMR Spectroscopy Studies in Solution**

As we recently reported, the closely related square allyl metallacycles $[\{Pd(\eta^3\text{-}2\text{-}Me\text{-}C_3H_4)\}_2(4\text{-}PPh_2py)_4\{M(dppp)\}_2](CF_3SO_3)_6$ feature a complex dynamic behaviour due to an exchange process with their building blocks in solution. The rate of this process was found to be dependent both on the solvent and on the electronic and/or steric nature of the different building blocks.[9a]

Similarly, the crown-like macrocyclic species described in this work $[\{Pd(\eta^3\text{-}2\text{-}Me\text{-}C_3H_4)\}_6(4\text{-}PPh_2py)_{12}\{M_2(tpbz)\}_3](X)_{18}$ also display such an exchange with the $\{Pd(\eta^3\text{-}2\text{-}Me\text{-}C_3H_4)(4\text{-}PPh_2py)_2\}_2^-$ units (see NOESY showing the dynamic exchange between **3a$_6$3Pd$_3$** and **3a** in Figure S50), implying the concomitant cleavage of the Pd or Pt – pyridine bond. In this case, the rate of exchange is faster than that observed in the square-like metallacycles. All the synthesized assemblies showed broad or very broad signals for α-pyridine proton nuclei, their shape and shift being dependent on the counteranion and metal centre (Figure 4 and Table 1 for M = Pd and Figure 5 and Table 2 for M = Pt). Given the low symmetry of the system, in the slow exchange regime, two different $^1$H NMR peaks should be observed for both the α and β pyridine protons.

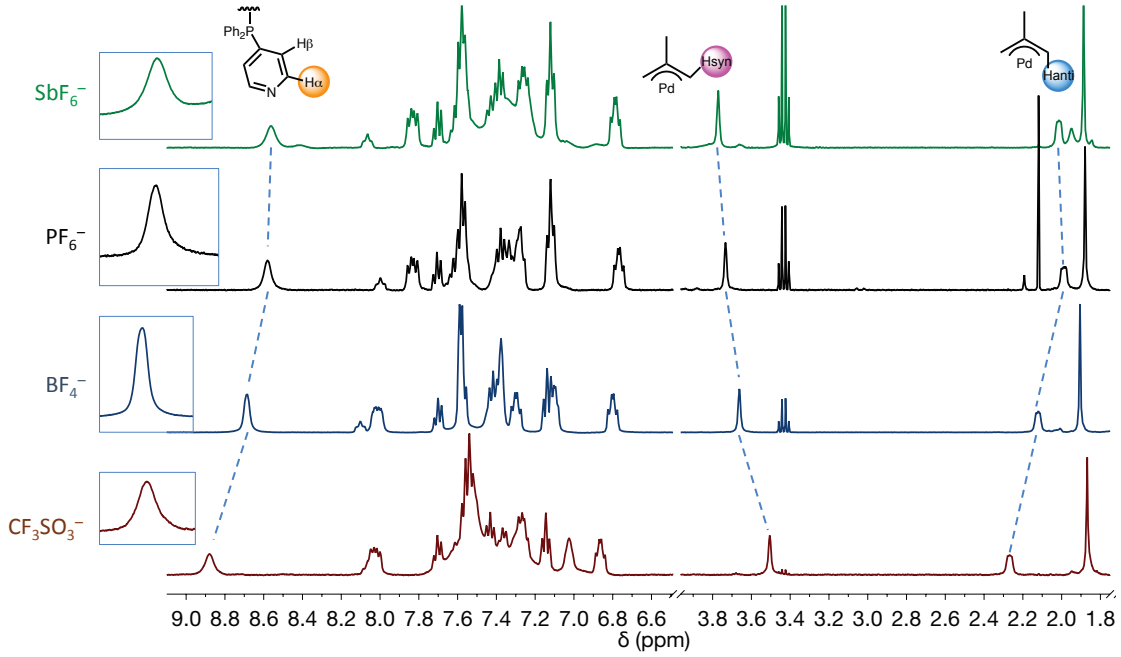


**Figure 4.** $^{1}$H NMR spectra of the $[\{Pd(\eta^3\text{-}2\text{-}Me\text{-}C_3H_4)\}_6(4\text{-}PPh_2py)_{12}\{Pd_2(tpbz)\}_3]^{18+}$ crown metallamacrocycles with different counteranions in $CD_2Cl_2$ at room temperature.

| Pd Crown | Counteranion | $\delta_{(ppm)}H_{\alpha\text{-py}}$ | $\delta_{(ppm)}H_{syn}$ allyl | $\delta_{(ppm)}$ $H_{anti}$ allyl |
|---|---|---|---|---|
| **$1a_6$1Pd$_3$** | $CF_3SO_3^-$ | 8.88 | 3.51 | 2.27 |
| **$2a_6$2Pd$_3$** | $BF_4^-$ | 8.69 | 3.66 | 2.13 |
| **$3a_6$3Pd$_3$** | $PF_6^-$ | 8.58 | 3.74 | 1.99 |
| **$4a_6$4Pd$_3$** | $SbF_6^-$ | 8.56 | 3.77 | 2.01 |

**Table 1**. $^{1}$H NMR molecular shifts of the significant resonances of the $[\{Pd(\eta^3\text{-}2\text{-}Me\text{-}C_3H_4)\}_6(4\text{-}PPh_2py)_{12}\{Pd_2(tpbz)\}_3]^{18+}$ crown-like metallamacrocycles with different counteranions in $CD_2Cl_2$ at room temperature.

A first inspection of the spectra in figures 4 and 5 clearly indicates that the homometallic $Pd_{12}$ species display a faster dynamic process than the closely related heterometallic $Pt_6Pd_6$ metallacycles, which is in agreement with the higher lability of the $Pd^{II}$ centre. In fact, as it can be observed in the expansion in Fig. 5, the α-pyridine protons of heterometallic species appear as very broad peaks (in the case of $SbF_6^-$ species the signal seems to be near to the coalescence temperature).

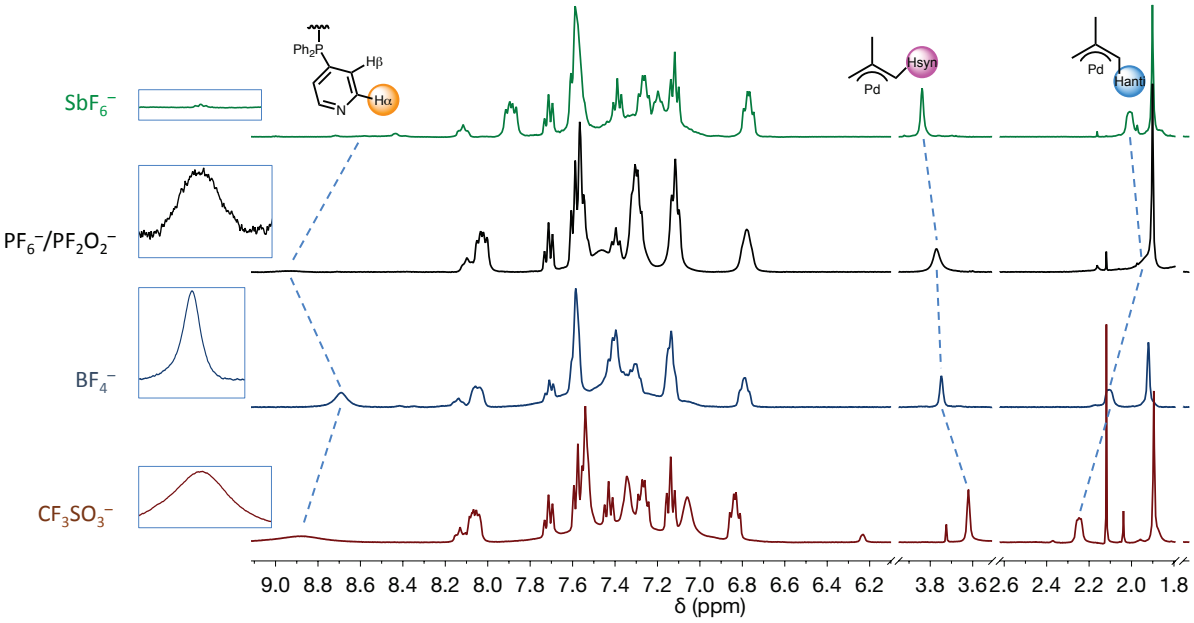


**Figure 5.** $^{1}$H NMR spectra of the [{Pd($\eta^3$-2-Me-$C_3H_4$)}$_6$(4-PPh$_2$py)$_{12}${Pt$_2$(tpbz)}$_3$]$^{18+}$ crown metallamacrocycles with different counteranions in $CD_2Cl_2$ at room temperature.

| Pt Crown | Counteranion | $\delta_{(ppm)}H_{\alpha\text{-py}}$ | $\delta_{(ppm)}H_{syn}$ allyl | $\delta_{(ppm)}$ $H_{anti}$ allyl |
|---|---|---|---|---|
| **1a$_6$1Pt$_3$** | $CF_3SO_3^-$ | 8.89 | 3.62 | 2.25 |
| **2a$_6$2Pt$_3$** | $BF_4^-$ | 8.69 | 3.75 | 2.10 |
| **3a$_6$3Pt$_3$** | $PF_6^-$/$PF_2O_2^-$ | 8.95 | 3.77 | 1.90 |
| **4a$_6$4Pt$_3$** | $SbF_6^-$ | 9.00-8.40 | 3.84 | 2.01 |

**Table 2**. $^{1}$H NMR chemical shifts of the significant resonances of the [{Pd($\eta^3$-2-Me-$C_3H_4$)}$_6$(4-PPh$_2$py)$_{12}${Pt$_2$(tpbz)}$_3$]$^{18+}$ crown metallamacrocycles with different counteranions in $CD_2Cl_2$ at room temperature

From the data it is clear that the nature of the counteranion has a dramatic effect on both the chemical shifts and the broadness of the α-py signals. The narrowest resonance is observed for the $BF_4^-$ compounds (indicative of a faster exchange), and a noticeable downfield shift is observed for the $CF_3SO_3^-$ derivatives. Interestingly, in spite of the fluxionality of the unassembled allyl-Pd unit, very little differences in the shape or value of chemical shifts of the allyl signals are observed once incorporated in the metallomacrocycles, which is in line with the lack of involvement of the allyl-Pd bond

of the assemblies in their dynamic process. This behaviour has been also found in the closely related tetranuclear allylic assemblies reported by us.[9a]

### $^{19}$F NMR Spectroscopy Studies in Solution

In order to investigate the existence of weak interactions between the fluorinated anions and the reported assemblies that could contribute to account for the observed differences, the study of their $^{19}$F NMR spectra of at 298K was carried out (see Figures 6 and S52). For $[\{Pd(\eta^3\text{-}2\text{-}Me\text{-}C_3H_4)\}_6(4\text{-}PPh_2py)_{12}\{M_2(tpbz)\}_3](BF_4)_{18}$ (M = Pd, **2a$_6$2Pd$_3$**; Pt, **2a$_6$2Pt$_3$**), the spectra showed two different resonances at δ ≈ -151 and -147 ppm ascribed to free and enclosed $BF_4^-$ anions.[16a, 23] Hexafluorophosphate derivatives $[\{Pd(\eta^3\text{-}2\text{-}Me\text{-}C_3H_4)\}_6(4\text{-}PPh_2py)_{12}\{Pd_2(tpbz)\}_3](PF_6)_{18}$ (**3a$_6$3Pd$_3$**) and $[\{Pd(\eta^3\text{-}2\text{-}Me\text{-}C_3H_4)\}_6(4\text{-}PPh_2py)_{12}\{Pt_2(tpbz)\}_3](PF_6)_6(PF_2O_2)_{12}$ (**3a$_6$5Pt$_3$**) also display two $^{19}$F NMR signals at δ ≈ -72 (less intense) and -68 ppm with a $J(^{31}P\text{-}^{19}F)$ ≈ 714 Hz, thus indicating a similar situation. For both $BF_4^-$ and $PF_6^-$ assemblies the low intensity resonances are downfield shifted by Δδ ≈ 4 ppm, which is indicative of the existence of enclosed anions interacting with the crown metallacyclophane edges. The $^{19}$F NMR spectra of the $SbF_6^-$ derivatives **4a$_6$4Pd$_3$** and **4a$_6$4Pt$_3$** showed two poorly defined (most probably due to the very large NMR line widths arising from the quadrupole relaxation of the Sb nuclei and/or the interacting and free anion exchange) signals δ ≈ -121 and -114 ppm.[22]

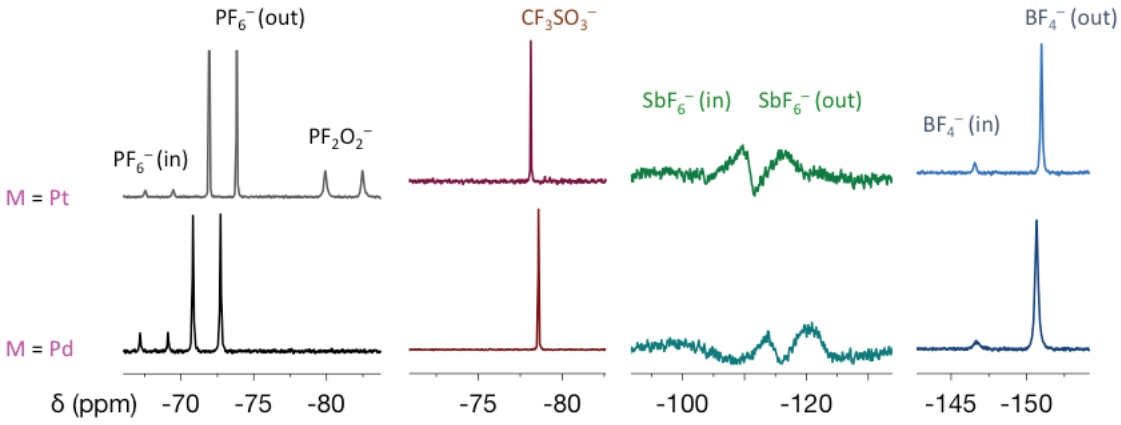


**Figure 6.** $^{19}$F NMR spectra of the $[\{Pd(\eta^3\text{-}2\text{-}Me\text{-}C_3H_4)\}_6(4\text{-}PPh_2py)_{12}\{Pd_2(tpbz)\}_3]^{18+}$ crown metallamacrocycles with different counteranions in $CD_2Cl_2$ at room temperature.

In contrast, the triflate derivatives **1a$_6$1Pd$_3$** and **1a$_6$1Pt$_3$** exhibited only a single $^{19}$F NMR resonance at δ ≈ -78 ppm that does not suffer any variation on performing NMR variable-temperature experiments. Analogously, only one signal at -81.2 ppm ($J$($^{31}$P-$^{19}$F)= 962 Hz) is observed for the oxygen-containing $PF_2O_2^-$ anion in the **3a$_6$5Pt$_3$** compound. These observations could be compatible either with a very fast enclosed/free exchange equilibrium process or with the fact that these anions are not confined within the cavity of the metallacycles.

**Other NMR Studies**

After the amazing impossibility of obtaining the $PF_6^-$ heterometallic "**3a$_6$3Pt$_3$**" metallamacrocycle in spite of the close similarity with other anions used in this work, we decided to further investigate the effect of the presence of a mixture of anions on the self-assembly process. For this purpose, a series of small-scale self-assembly reactions combining some of the available building blocks *i. e.* [{Pd(η$^3$-2-Me-$C_3H_4$)(4-$PPh_2py)_2$}$_2$]X (X = $BF_4^-$, $PF_6^-$, $SbF_6^-$, $CF_3SO_3^-$, $BArF^-$) and [$M_2$(tpbz)(solvent)$_4$]$X_4$ (M = Pd, Pt; (X = $BF_4^-$, $PF_6^-$, $SbF_6^-$, $CF_3SO_3^-$) were performed. The reactions were monitored by $^1$H and $^{31}$P{$^1$H} NMR spectroscopy after mixing the appropriate quantities of the precursors in $CD_2Cl_2$ at room temperature. A summary of the results is indicated below:

a) The mixtures do not produce a single symmetrical species when each of the building blocks has a different counteranion.

b) When the $PF_6^-$ salt of the allyl-Pd moiety is combined with [$M_2$(tpbz)(solvent)$_4$]($BF_4$) a mixture of a limited number of assemblies is obtained that can not be ascribed to any of the above reported crown-like macrocyclic species. Experiments involving [{Pd(η$^3$-2-Me-$C_3H_4$)(4-$PPh_2py)_2$}$_2$]$BF_4$ and [$M_2$(tpbz)(solvent)$_4$]($SbF_6$)$_4$ gave analogous results.

c) All the attempts to use the $PF_6^-$ salt of the Pt$^{II}$ acceptor moiety [$Pt_2$(tpbz)(solvent)$_4$]($PF_6$)$_4$ as a building block only lead to the formation of oligomeric mixtures as observed in the self-assembly reaction using only hexafluorophosphate as counteranion under strictly dry conditions (see above).

Given the surprising fact that $PF_6^-$ precludes the self-assembly of the Pt$^{II}$ crown supramolecules, we studied the reaction of a mixture of [Pd(η$^3$-2-Me-$C_3H_4$)(4-$PPh_2py)_2$]$PF_6$ and [$Pt_2$(tpbz)(solvent)$_4$]($PF_6$)$_4$ with a 5 fold excess of $Bu_4NBF_4$ in $CD_2Cl_2$ at room temperature. The monitoring of the reaction by $^{31}$P{$^1$H} NMR spectroscopy during 2 days showed no changes in the recorded spectra, thus evidencing that the $BF_4^-$

compound had not been assembled even in the presence of a large excess of the latter anion. Likewise, the mirror experiment was also conducted, *i. e.* a 5 fold excess of $Bu_4NPF_6$ was added to a $CD_2Cl_2$ solution of $[Pd(\eta^3\text{-}2\text{-}Me\text{-}C_3H_4)(4\text{-}PPh_2py)_2]BF_4$ (**2a**) and $[Pt_2(tpbz)(solvent)_4](BF_4)_4$ (**2Pt**) in a 2:1 molar ratio. In this case, in spite the presence of the $PF_6^-$ anion, the $BF_4^-$ metallamacrocyle $\mathbf{2a_6 2Pt_6}$ was obtained, as could be evidenced by NMR spectroscopy. Adding up, the results reported here reinforce the determining role of the nature of counteranions in the course of self-assembly processes. Related observations have been reported for Dunbar and col. when studying the self-assembly between different M(II) cations and the 3,6-bis(2-pyridyl)-1,2,4,5-tetrazine ligand (bptz).[16a, 23]

**Theoretical Studies**

DFT calculations have been employed to study the intermolecular interaction in the above reported crown-like complexes (see Computational details in Supp. Information for a description of the employed methodology). The first step was to analyse the electrostatic potential of the empty $[\{Pd(\eta^3\text{-}2\text{-}Me\text{-}C_3H_4)\}_6(4\text{-}PPh_2py)_{12}\{Pt_2(tpbz)\}_3]^{18+}$ crown (see Figure 7). The electrostatic potential shows that the high positive charge of this crown-like structure is mainly localized in the internal part of the crown. Hence, this internal region is specially appropriated for the establishment of interaction with anions. The number of anions within the cavity is limited to six due to the cavity size inferred from the X-ray diffraction structure of $\mathbf{3a_6 5Pt_3}$. Interestingly, an inspection of the representation of the electrostatic potential shows the existence of six " positive pockets" inside the cavity, appropriate to accommodate them. Moreover, a larger number of anions will result in huge anion-anion repulsions.

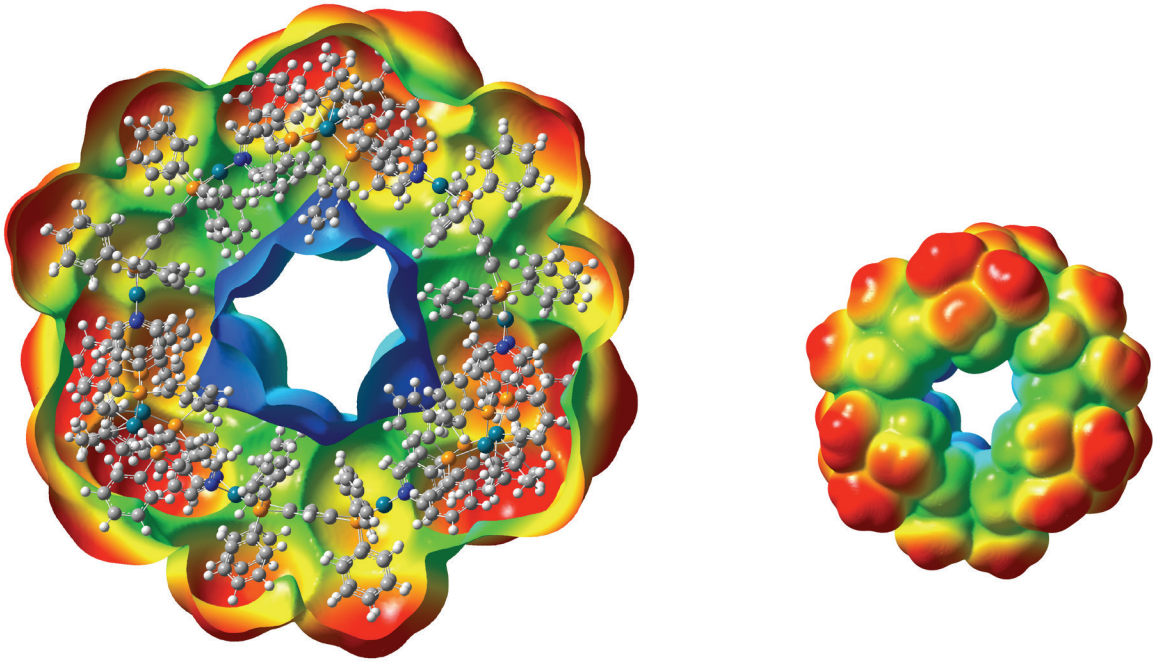

**Figure 7.** Representations of the electrostatic potential of the empty [{Pd($\eta^3$-2-Me-$C_3H_4$)}$_6$(4-PPh$_2$py)$_{12}${Pt$_2$(tpbz)}$_3$]$^{18+}$ crown calculated at B3LYP level.

The optimized structures for the Pt systems with four different counteranions (6 $BF_4^-$, 6 $PF_6^-$, 3 $PF_6^-$/3 $PF_2O_2^-$ and 6 $CF_3SO_3^-$) are represented in Figure 8. In agreement with the X-ray data of **3a$_6$5Pt$_3$** (see Figure 6) the six anions are placed close to the $Pt^{II}$ and $Pd^{II}$ cations. In the case of $PF_2O_2^-$ and $CF_3SO_3^-$, the negative charge is mainly localized on the oxygen atoms that are closer to the crown metal centers than the fluorine atoms. In all cases, the six enclosed anions are quite close to the metal cations with fluorine-metal and oxygen-metal distances being around 2.4-2.5 and 2.7-2.8 Å, respectively. The calculated anion-crown interaction energies at B3LYP level are collected in Table 3. The results indicate that the interactions with the homometalllic $Pd_{12}$ systems are slightly stronger than those of the corresponding $Pd_6Pt_6$ metallamacrocycles. The average anion-crown interactions involving anions without oxygen atoms ($BF_4^-$ and $PF_6^-$) are stronger than that of $PF_2O_2^-$ and $CF_3SO_3^-$, being the strongest interaction with $PF_6^-$. On the other hand, the repulsion energies between the anions (see Table 3) are relatively similar independently of the nature of the anion being the weakest ones those corresponding to $CF_3SO_3^-$ systems.

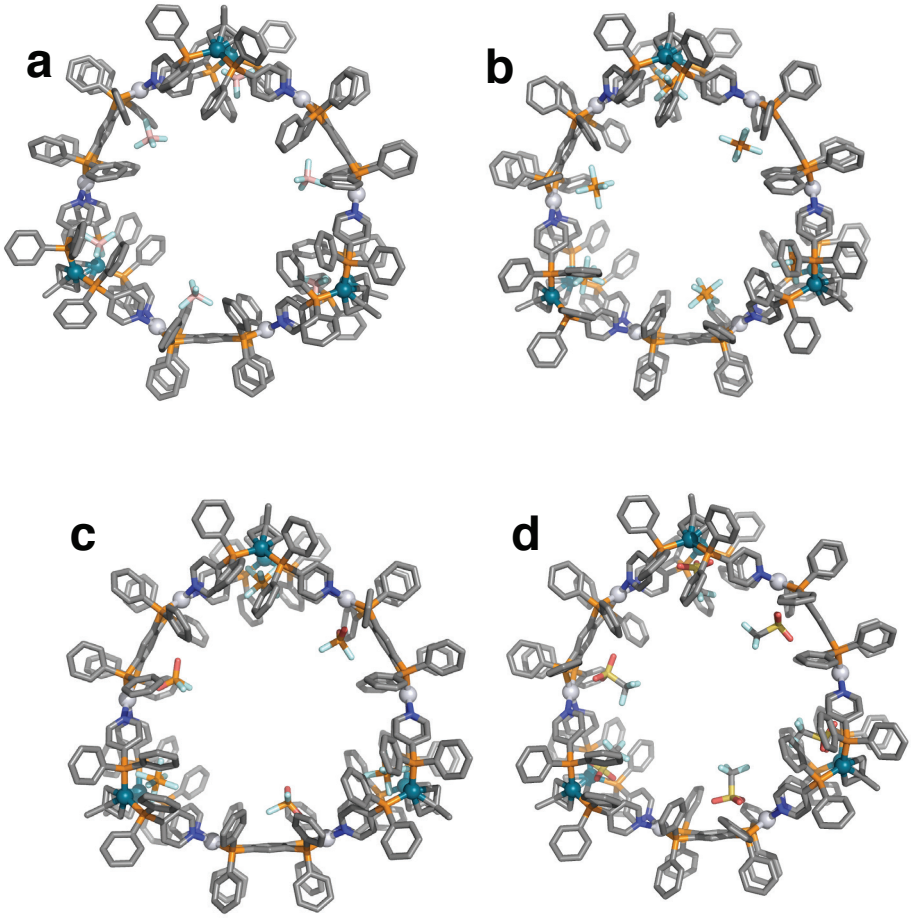


**Figure 8.** Representation of the four optimized crown structures of [{Pd($\eta^3$-2-Me-$C_3H_4$)}$_6$(4-PPh$_2$py)$_{12}$}{Pt$_2$(tpbz)}$_3$]$^{18+}$ with (a) 6 $BF_4^-$, (b) 6 $PF_6^-$, (c)3 $PF_6^-$·3 $PF_2O_2^-$ and (d) 6 $CF_3SO_3^-$ anions using the GFN2-xTB method (see Computational details). Gray and blue sphere correspond to $Pt^{II}$ and $Pd^{II}$ centers and pink, gray, blue, red, light blue, orange and yellow wires represent boron, carbon, nitrogen, oxygen, fluorine, phosphorus and sulphur atoms. Cartesian coordinates of equivalent structure only with $Pd^{II}$ cations are provided as SI.

| M and anion-type | $E_{rep}$ | $E_{int}$ |
|---|---|---|
| **Pd $BF_4^-$** | 45.4 | -54.8 |
| **Pd $PF_6^-$** | 46.4 | -66.8 |
| **Pd $PF_6^-$ $PF_2O_2^-$** | 45.8 | -49.7 |
| **Pd $CF_3SO_3^-$** | 43.2 | -51.0 |
| **Pt $BF_4^-$** | 45.4 | -53.6 |
| **Pt $PF_6^-$** | 46.0 | -58.7 |
| **Pt $PF_6^-$ $PF_2O_2^-$** | 45.0 | -47.0 |
| **Pt $CF_3SO_3^-$** | 43.6 | -49.0 |

**Table 3**. Interaction energies (in kcal/mol) at B3LYP level for the [{Pd($\eta^3$-2-Me-$C_3H_4$)}$_6$(4-$PPh_2$py)$_{12}${$M_2$(tpbz)}$_3$]$^{18+}$ (X: $Pd^{II}$ and $Pt^{II}$) crown metallamacrocycles with 6 $BF_4^-$, 6 $PF_6^-$, 3 $PF_6^-$/3 $PF_2O_2^-$ and 6 $CF_3SO_3^-$ anions. The repulsion energy ($E_{rep}$) between the six anions calculated as the energy difference between the system with six anions together and the six isolated molecules while the average crown-anion interactions per anion ($E_{int}$) are obtained as the energy difference between the total system with respect to the crown and the isolated anions.

The fact that the anions without oxygen atoms have the strongest anion-crown interaction energies is in agreement with the $^{19}$F NMR spectra where signals arising from both enclosed and free $BF_4^-$, $PF_6^-$ and $SbF_6^-$ anions can be clearly seen (Figure 5). On the contrary, the less tightly bound $PF_2O_2^-$ and $CF_3SO_3^-$ are involved faster in-out equilibria giving rise to a single peak even in the presence of a perfluorinated anion (compound **$3a_6$5$Pt_3$**). Moreover, the observed difference between the type of interactions involving oxygen fluoroanions and that of the anions without oxygen atoms could explain the difference in the chemical shifts observed in the $^1$H NMR spectra (Figures 3 and 4) for the close to metal α-pyridine protons.

**Preliminary Catalytic Studies**

Phosphanes are excellent ligands in palladium-catalysed allylic substitution reactions.[10a] Although this reaction has been widely studied for a large variety of $Pd^{II}$-based catalysts, it is well known that the activity is strongly dependent on several

parameters including the structure of the allylic substrate, the nucleophile, and even the solvent used.[10c, 24] In contrast, the regioselectivity of the allylic alkylation is mainly controlled by the nature of the ligands. Hence, in general symmetrical diphosphanes favour the substitution at the terminal carbon atom, leading to the linear (achiral) substituted product,[25] while the use of bulkier ligands switch the selectivity towards the branched product.[26]

Supramolecular assemblies containing catalytically active allyl-$Pd^{II}$ units represent a promising approach for the study of the regioselectivity of these transformations. Despite that each metallic centre contains monodentate ligands, the geometry and the rigidity of the system confers properties usually associated to bidentate chelating systems.[27]

In this respect, we previously reported the preparation of a square allyl-cornered metallacycle that proved active in the allylic alkylation reaction of cinnamyl acetate.[9a] In our efforts to increase the nuclearity and regarding the possibility of cooperative effects that might lead to unexpected activities and selectivities,[28] we have studied the catalytic behaviour of the supramolecular crowns prepared in this work in the allylic alkylation reaction of 3-acetoxy-1-phenyl-1-propene with $CH_2(COOMe)_2$ as nucleophile in $CH_2Cl_2$ under the well-known Trost conditions (AG1) using *N*,*O*-bis(trimethylsilyl)acetamide (BSA) and potassium acetate. The reaction has been performed at room temperature and with a 0.5 mol% of concentration level of catalyst (Scheme 2). A blank study by using the corresponding mononuclear palladium corners has also been conducted for comparative purposes. Results have been collected in Table 4.

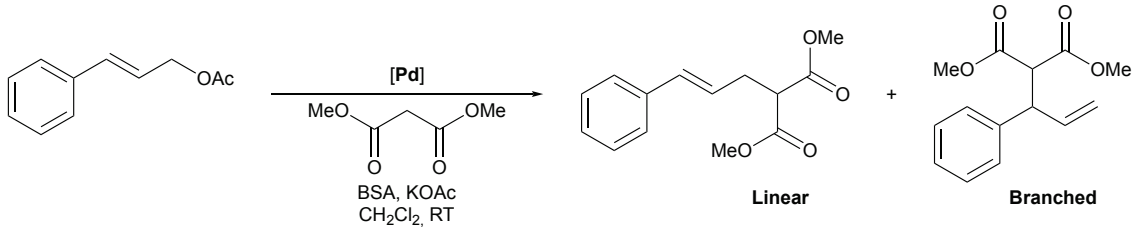


**Scheme 2**. Pd-catalysed allylic alkylation of 3-acetoxy-1-phenyl-1-propene.

**Table 4.** Catalytic results of the allylic alkylation of 3-acetoxy-1-phenyl-1-propene according to Scheme 2.[a]

| Entry | Precursor | Time | Conversion [%] | Branched/Linear |
|---|---|---|---|---|
| 1 | **1a** | 1 h | >99 | 1:8 |
| 2 | **$1a_6$1Pd$_3$** | 24 h | 70 | All linear |
| 3 | **$1a_6$1Pt$_3$** | 24 h | 20 | All linear |
| 4 | **2a** | 1 h | >99 | 1:6 |
| 5 | **$2a_6$2Pd$_3$** | 24 h | 80 | All linear |
| 6 | **$2a_6$2Pt$_3$** | 24 h | <1 | All linear |
| 7 | **3a** | 1 h | >99 | 1:12 |
| 8 | **$3a_6$3Pd$_3$** | 24 h | >99 | All linear |
| 9 | **$3a_6$5Pd$_3$** | 24 h | nd[b] | nd |
| 10 | **4a** | 1 h | >99 | 1:7 |
| 11 | **$4a_6$4Pd$_3$** | 24 h | >99 | All linear |
| 12 | **$4a_6$4Pt$_3$** | 24 h | 50 | 1:27 |
| 13 | **5a** | 1 h | 10 | All linear |

[a] Catalytic conditions: 1 mmol substrate, 3 mmol dimethyl malonate, 3 mmol BSA, 0.01 mmol KOAc, 4 mL $CH_2Cl_2$, RT. Conversion and branched:linear ratio determined by GC.

[b]. No determined. The crown contained a mixture of $PF_6^-$ and $PO_2F_2^-$ anions.

Complete conversions and branched/linear product ratios of the alkylation ranging from 1:6 to 1:99 were obtained after one hour of reaction when the mononuclear corners were used as catalytic precursors, as found for analogous allylic compounds[25] $[Pd(\eta^3\text{-}C_3H_5)(PPh_3)_2]^+$. Interestingly, the increase of the bulkiness of the fluorinated counteranion affects the regioselectivity of the reaction leading to the linear product exclusively, as observed for the $BArF^-$ corner.

Our previous catalytic studies of this reaction using square allyl-cornered metallacycles showed that the presence of the nitrogen donor in the phosphane ligands did not play any relevant role neither on the regioselectivity nor on the activity of the alkylation, a trend also observed with the supramolecular assemblies described in this work. However, the prepared crowns displayed a better regioselectivity compared to its related metallacyclic squares, affording exclusively the linear alkylated product after 24 h, a fact that might be attributed to the more rigid environment in the supramolecular assembly. On moving to the results for the conversions of the Pd/Pd and Pd/Pt crowns, some differences are observed. Whereas the Pd/Pd catalysts have a more similar activity compared to its related mononuclear counterparts, heterometallic assemblies displayed lower activities, which paralleled to the behaviour observed for the previously studied tetranuclear species. Hence, the allylic fragment is less prone to a nucleophilic attack or an oxidative addition of the substrate than in the unassembled form, which in agreement with the less labile nature of the py-Pt bonds.

**Conclusions**

We have demonstrated that the self-assembly of $\{Pd(\eta^3\text{-}2\text{-}Me\text{-}C_3H_4)\}^+$, $\{M_2(tpbz)\}^{4+}$ ( M = Pd, Pt) and 4-$PPh_2$py moieties in 2:1:4 molar ratio produces quantitatively the highly positively charged crown-like metallacycles $[\{Pd(\eta^3\text{-}2\text{-}Me\text{-}C_3H_4)\}_6(4\text{-}PPh_2py)_{12}\{M_2(tpbz)\}_3]^{18+}$. These assemblies have been obtained in combination with different fluorinated counteranions that have conduced to the formation of single species having the same nuclearity than the indicated above. The presence of mixtures of anions in the self-assembly process does not allow the formation of single species and uncharacterizable mixtures are obtained, instead. The obtained metallamacrocycles are stereochemically non-rigid and their dynamic process that involves a coordination-decoordination of the M-py bond have, in addition to the higher lability of the $Pd^{II}$ cation, a remarkable dependence on the counteranion present in solution.

The large cavity of the synthesized metallacycles (evidenced by DFT and X-ray diffraction studies) has a high positive electrostatic potential in its centre whose representation displays six “pockets” where the accommodation of six anions is expected to fit. These six anions are involved in weak interactions with the metal centres through either their oxygen or fluorine atoms. DFT calculations have shown that the perfluorinated anions $BF_4^-$ and $PF_6^-$ interact more strongly with the metallic centres

than the anions that bear oxygen atoms ($CF_3SO_3^-$, $PF_2O_2^-$). These differences in strength and/or character of the anion-crown interactions are in agreement with relevant facts evidenced by NMR spectroscopy.

The experiments carried out clearly supports the contention that the anions play a decisive role in the formation and stability of complex architectures and provide unequivocal proof of a template effect only in the presence of specific anions.

Although the new palladium crown-like metallamacrocycles are active catalysts in the allylic alkylation reaction of 3-acetoxy-phenyl-1-propene, the regioselectivity of the catalytic process do not show significant differences in comparison with that of the related catalytically active species of lesser nuclearity. Moreover, the increase of the bulkiness of the fluorinated counteranion affects the regioselectivity of the reaction leading to the linear product exclusively.

Finally, the construction of bigger and more complicated metallamacrocycles bearing larger cavities that can establish interactions with a wide range of anions through the design of new ligands is currently under investigation.

## Experimental Section

### General Methods

All manipulations were performed under prepurified $N_2$ using standard Schlenk techniques. Solvents were dried by standard methods and distilled under nitrogen immediately prior to use, or alternatively from a Solvent Purification System (Innovative Technologies).

Infrared spectra were recorded on an FT-IR 5700 Nicolet spectrophotometer. $^{31}P\{^1H\}$-NMR ($\delta$(85% $H_3PO_4$) = 0.0 ppm), $^1$H-NMR ($\delta$(TMS) = 0.0 ppm) and $^{19}$F-NMR ($\delta(CFCl_3)$ = 0.0 ppm) spectra were obtained at 400 or 500 MHz with Varian and Bruker spectrometers at 25 ºC unless otherwise stated. Elemental analyses of C, H, N and S were carried out at the Centres Científics i Tecnològics (Universitat de Barcelona). ESI mass spectra were recorded on a Bruker APEX IV Fourier-transform ion cyclotron resonance mass spectrometer with a 7.05 T magnet and an Apollo electrospray ion source, a Q/TOF mass spectrometer (micrOTOF-Q from Bruker), a Thermo FisherScientific Orbitarp XL or on a LC/MSD-TOF instrument from Agilent Technologies. Unless otherwise state, acetone solutions of the analysed compounds (0.1-0.2 mM) were used with flow rates of

3-4 or 10 μLmin$^{-1}$ depending on the spectrometer used. In each case, ESI parameters were tuned for optimal signal intensities in order to minimize in source fragmentation.

The compounds [Pd(μ-Cl)($\eta^3$-2-Me-$C_3H_4$)]$_2$,[29] [Pd($\eta^3$-2-Me-$C_3H_4$)(COD)]X (X= $BF_4^-$, $OTf^-$, $PF_6^-$, $SbF_6^-$, BArF),[30] [Pd($\eta^3$-2-Me-$C_3H_4$)(4-$PPh_2$py)$_2$]($CF_3SO_3$),[9a] [$M_2Cl_4$(tpbz)] ( M = Pd, Pt),[12c] [$M_2$(tpbz)($CF_3SO_3$)$_4$] (M=Pd, Pt),[12c] 4-$PPh_2$py[31] and tpbz[32] were prepared as described previously. All other reagents were obtained from commercial suppliers and used as received.

**X-Ray structure determination**

Crystal data for complex **3a$_6$5Pt$_3$** are presented in the ESI (Table S1).

Data were collected at 100 K on a Bruker-Nonius FR591 KappaCCD2000 rotating anode diffractometer employing Cu $K\alpha$ radiation (λ = 1.54178 Å) monochromated using a multilayer confocal mirror. Data collection was done using the program Collect (Bruker AXS BV, 1997-2004) and data reduction was undertaken with HKL DENZO and SCALEPACK programs.[33] The structure was solved by direct methods (SHELXL) and refined by constrained full least-squares on $F^2$ with SHELXL-2012.(SHELXL2) The contribution of the disordered solvent molecules within the unit cells of the complex to the structure factors was taken into account by back-fourier transformation using the SQUEEZE algorithm(PG07) as implemented in PLATON.[34]

CCDC 1951512 contains the crystallographic data along with specific details pertaining to the refinement.

**Computational details**

The structure of the crown complexes was optimized by using the GFN2-xTB approach proposed by Grimme and coworkers.[35] The cartesian coordinates of the eight optimized structures are provided as SI. In the triflate systems, the interaction of the anions with the crown complexes was considered through the fluorine and oxygen atoms of such anion being more stable the interaction with the $SO_3$ group. The interaction energies were calculated with those optimized structures by using the B3LYP exchange correlation functional[36] implemented in the Gaussian09 code[37] with the LanL2DZ basis set including pseudopotentials for the metal centres. The solvent effects (dichloromethane) were included with the polarizable conductor calculation model.[38] The interaction energies were calculated using the energy of the full system with the six anions and the

energies of each isolated anion and the crown complex. For one of the complexes $Pd_{12}$·6$BF_4$ the basis set superposition error was estimated performing the calculations without the solvent contribution being around 3% of the total interaction. Such error is rather small because the anion···crown complex is relatively strong due to a large electrostatic contribution.

**Synthesis and characterization**

Synthesis of [Pd($\eta^3$-2-Me-$C_3H_4$)(4-$PPh_2$py)$_2$]$BF_4$ (**2a**)

Solid 4-$PPh_2$py (100 mg, 0.38 mmol) was added to a dichloromethane solution (10 mL) of [Pd($\eta^3$-2-Me-$C_3H_4$)(COD)]$BF_4$ (68 mg, 0.19 mmol) at room temperature. After 30 min of stirring, the reaction mixture was filtered, concentrated to *ca*. half volume under vacuum and precipitated with diethyl ether. An off-white crystalline solid was obtained in 80% yield (118 mg). $^1$H NMR (400 MHz, $CDCl_3$): δ = 8.43 (dd, $J_1$ = 4.3 Hz, $J_2$ = 1.9 Hz, 4H, $H_{\alpha\text{-py}}$), 7.52-7.36 (m, 20H, Ph), 6.98 (d, *J*= 4.3 Hz, 4H, $H_{\beta\text{-py}}$), 3.96 (s br, 2$H_{syn}$, Me-$C_3H_4$), 3.72 (s, 2$H_{anti}$, Me-$C_3H_4$), 1.87 (s, 3H, *Me*-$C_3H_4$). $^{31}$P{$^1$H} NMR (161.9 MHz, $CDCl_3$): δ = 22.5 (s). $^{19}$F NMR (376 MHz, $CDCl_3$): δ = 151.2 (s, $^{10}BF_4$), 151.3 (s,$^{11}BF_4$). IR (KBr disk): $\tilde{\nu}$ = 1573, 1479, 1436, 1083, 1060, 1034. ESI(+) LC/MSD-TOF *m/z*: 687.1316 [**2a**-$BF_4$]$^+$; calcd: 687.1319; 424.0454 [**2a**-4-$PPh_2$py-$BF_4$]$^+$ ; calcd: 424.0455.

Compounds **3-5a** were synthesized following an analogous procedure to that described for compound **2a**.

Synthesis of [Pd($\eta^3$-2-Me-$C_3H_4$)(4-$PPh_2$py)$_2$]$PF_6$ (**3a**)

From (80 mg, 0.19 mmol) of [Pd($\eta^3$-2-Me-$C_3H_4$)(COD)]$PF_6$ compound **3a** was obtained as a white crystalline solid in 87% yield (140 mg). $^1$H NMR (400 MHz, $CDCl_3$): δ = 8.43 (m, 4H, $H_{\alpha\text{-py}}$), 7.53-7.38 (m, 20H, Ph), 6.93 (d, *J*= 5.9 Hz, 4H, $H_{\beta\text{-py}}$), 3.82 (s br, 2$H_{syn}$, Me-$C_3H_4$), 3.72 (s, 2$H_{anti}$, Me-$C_3H_4$), 1.89 (s, 3H, *Me*-$C_3H_4$). $^{31}$P{$^1$H} NMR (161.9 MHz, $CDCl_3$): δ = 22.6 (s, $PPh_2$py), -144.3 (sept, $J(^{31}P\text{-}^{19}F)$= 714 Hz, $PF_6$). $^{19}$F NMR (376 MHz, $CDCl_3$): δ = -72.17 (d, $J(^{31}P\text{-}^{19}F)$= 714 Hz, $PF_6$). IR (KBr disk): $\tilde{\nu}$ = 1575, 1480, 1435, 1100, 842. ESI(+) LC/MSD-TOF *m/z*: 687.1315 [**3a**-$PF_6$]$^+$; calcd: 687.1319; 424.0448 [**3a**-4-$PPh_2$py-$PF_6$]$^+$ ; calcd: 424.0455.

Synthesis of [Pd($\eta^3$-2-Me-$C_3H_4$)(4-$PPh_2$py)$_2$]$SbF_6$ (**4a**)

From (95 mg, 0.19 mmol) of [Pd($\eta^3$-2-Me-$C_3H_4$)(COD)]$SbF_6$ compound **4a** was obtained as pale yellow crystalline solid in 85% yield (150 mg). $^1$H NMR (400 MHz, $CDCl_3$): δ =

8.43 (s br, 4H, $H_{\alpha\text{-py}}$), 7.52-7.36 (m, 20H, Ph), 6.92 (s br, 4H, $H_{\beta\text{-py}}$), 3.73 (s br, $2H_{syn}$+$2H_{anti}$, Me-$C_3H_4$), 1.90 (s, 3H, *Me*-$C_3H_4$). $^{31}P\{^1H\}$ NMR (161.9 MHz, $CDCl_3$): δ = 24.9 (s). IR (KBr disk): $\tilde{\nu}$ = 1575, 1480, 1438, 1100, 659. ESI(+) LC/MSD-TOF *m/z*: 687.1307 [**4a**-$SbF_6$]$^+$; calcd: 687.1319; 424.0455 [**4a**-4-$PPh_2$py-$SbF_6$]$^+$ ; calcd: 424.0455.

Synthesis of [Pd(η$^3$-2-Me-$C_3H_4$)(4-$PPh_2$py)$_2$]BArF (**5a**)

From (215 mg, 0.19 mmol) of [Pd(η$^3$-2-Me-$C_3H_4$)(COD)]BArF compound **5a** was obtained as pale yellow crystalline solid in 70% yield (205 mg). $^1H$ NMR (400 MHz, $CDCl_3$): δ = 8.42 (s br, 4H, $H_{\alpha\text{-py}}$), 7.70 (m, 8H, $H_{BArF}$), 7.52-7.50 (m, 8H, $H_{BArF}$+ $H_{p\text{-Ph}}$), 7.36 (m, 8H, $H_{m\text{-Ph}}$), 7.26 (m, 8H, $H_{o\text{-Ph}}$), 6.79 (m, 4H, $H_{\beta\text{-py}}$), 3.75 (s br, $2H_{syn}$, Me-$C_3H_4$), 3.24 (m, $2H_{anti}$, Me-$C_3H_4$), 1.87 (s, 3H, *Me*-$C_3H_4$). $^{31}P\{^1H\}$ NMR (161.9 MHz, $CDCl_3$): δ = 23.4 (s). $^{19}F$ NMR (376 MHz, $CDCl_3$): δ = -62.41 (s, BArF). IR (KBr disk): $\tilde{\nu}$ = 1587, 1482, 1440, 1356, 1279, 1125. ESI(+) LC/MSD-TOF *m/z*: 687.1329 [**5a**-BArF]$^+$; calcd: 687.1319; 424.0452 [**5a**-4-$PPh_2$py-BArF]$^+$ ; calcd: 424.0455.

Synthesis of [$Pd_2$(tpbz)(solvent)$_4$] ($BF_4$)$_4$ (**2Pd**)

Solid $AgBF_4$ (80 mg, 0.41 mmol) was added to a dichloromethane/acetonitrile (20:20ml) suspension of [$Pd_2Cl_4$(tpbz)] (116 mg, 0.10 mmol) at room temperature. After stirring in the dark overnight, the reaction mixture was filtered, concentrated to 5 ml under vacuum and precipitated with 30 ml of diethyl ether. A white solid was obtained in 68% yield (105 mg) (considering the isolation of [$Pd_2$(tpbz)($CH_3CN$)$_4$]($BF_4$)$_4$). $^1H$ NMR (400 MHz, $CD_3NO_2$): δ = 8.34 (m, 2H, $C_6H_2P_4$), 7.83-7.74 (m, 24H, Ph), 7.65-7.60 (m, 16H, Ph). $^{31}P\{^1H\}$ NMR (161.9 MHz, $CD_3NO_2$): δ = 66.0 (s). $^{19}F$ NMR (376 MHz, $CD_3NO_2$): δ = -154.9 (s, $^{10}BF_4$), -155.0 (s, $^{11}BF_4$). IR (KBr disk): $\tilde{\nu}$ = 2315, 2289,1482, 1438, 1083, 1060, 995. ESI(+) Orbitrap *m/z*: 590.02 [**2Pd**-2$CH_3CN$+2Cl-4$BF_4$]$^{2+}$; calcd: 590.01; 395.37 [**2Pd**-$CH_3CN$+Cl-4$BF_4$]$^{3+}$; calcd: 395.36; 387.69 [**2Pd**-2$CH_3CN$+$H_2O$+Cl-4$BF_4$]$^{3+}$; calcd: 387.69; 381.69 [**2Pd**-2$CH_3CN$+Cl-4$BF_4$]$^{3+}$; calcd: 381.69; 292.04 [**2Pd**-4$BF_4$]$^{4+}$; calcd: 298.04.; 298.28 [**2Pd**-$CH_3CN$+$H_2O$-4$BF_4$]$^{4+}$; calcd: 292.28.

Compounds **3Pd-4Pd** and **2Pt-5Pt** were synthesized following an analogous procedure to that described for compound **2Pd**.

Synthesis of [$Pd_2$(tpbz)(solvent)$_4$]($PF_6$)$_4$ (**3Pd**)

From 100 mg (0.40 mmol) of $AgPF_6$ and 116 mg (0.10 mmol) [$Pd_2Cl_4$(tpbz)] compound **3Pd** was obtained as white solid in 73% yield (130 mg) (considering the isolation of [$Pd_2$(tpbz)($CH_3CN$)$_4$]($PF_6$)$_4$). $^1H$ NMR (400 MHz, $CD_3CN$): δ = 7.94 (br, 2H, $C_6H_2P_4$),

7.70-7.65 (m, 24H, Ph), 7.53-7.49 (m, 16H, Ph). $^{31}P\{^{1}H\}$ NMR (161.9 MHz, $CD_3CN$): δ = 64.0 (s br, tpbz), -144.6 (sept, $J(^{31}P\text{-}^{19}F)$ = 706 Hz, $PF_6$). $^{19}F$ NMR (376 MHz, $CD_3CN$): δ = -72.95 (d, $J(^{31}P\text{-}^{19}F)$ = 706 Hz, $PF_6$). IR (KBr disk): $\tilde{\nu}$ = 2325, 2295, 1482, 1438, 1099, 837. ESI(+) Orbitrap *m/z*: 590.02 [**3Pd**-2$CH_3CN$+2Cl-4$PF_6$]$^{2+}$; calcd: 590.01; 578.51 [**3Pd**-3$CH_3CN$+$H_2O$+2Cl-4$PF_6$]$^{2+}$; calcd: 578.50; 569.50 [**2Pd**-3$CH_3CN$+2Cl-4$PF_6$]$^{2+}$; calcd: 569.50; 548.99 [**3Pd**-4$CH_3CN$+2Cl-4$PF_6$]$^{2+}$; calcd: 548.99.

Synthesis of $[Pd_2(tpbz)(solvent)_4](SbF_6)_4$ (**4Pd**)

From 140 mg (0.41 mmol) of $AgSbF_6$ and 116 mg (0.10 mmol) $[Pd_2Cl_4(tpbz)]$ compound **4Pd** was obtained as yellow solid in 78% yield (160 mg) (considering the isolation of $[Pd_2(tpbz)(H_2O)_4](SbF_6)_4$). $^{1}H$ NMR (400 MHz, $CD_3CN$): δ = 7.93 (br, 2H, $C_6H_2P_4$), 7.70-7.65 (m, 24H, Ph), 7.52-7.50 (m, 16H, Ph). $^{31}P\{^{1}H\}$ NMR (161.9 MHz, $CD_3CN$): δ = 64.1 (s br, tpbz). $^{19}F$ NMR (376 MHz, $CD_3CN$): δ = -123.8 (six, $J(^{121}Sb\text{-}^{19}F)$ = 1940 Hz; oct, $J(^{123}Sb\text{-}^{19}F)$ = 1050 Hz, $SbF_6$). IR (KBr disk): $\tilde{\nu}$ = 1482, 1438, 1100, 658. ESI(+) LC/MSD-TOF (acetone) *m/z*: 257.006 [**4Pd**-4$H_2O$-4$SbF_6$]$^{4+}$; calcd: 257.008. ESI(+) Orbitrap (acetonitrile) *m/z*: 589.96 [**4Pd**-4$H_2O$+2$CH_3CN$+2Cl-4$SbF_6$]$^{2+}$; calcd: 590.01; 569.44 [**4Pd**-4$H_2O$+$CH_3CN$+2Cl-4$SbF_6$]$^{2+}$; calcd: 569.50; 548.93 [**4Pd**-4$H_2O$+2Cl-4$SbF_6$]$^{2+}$; calcd: 548.99; 395.32 [**4Pd**-4$H_2O$+3$CH_3CN$+Cl-4$SbF_6$]$^{3+}$; calcd: 395.36.

Synthesis of $[Pt_2(tpbz)(solvent)_4](BF_4)_4$ (**2Pt**)

From 80 mg (0.41 mmol) of $AgBF_4$ and 135 mg (0.10 mmol) of $[Pt_2Cl_4(tpbz)]$ compound **2Pt** was obtained as white solid in 75% yield (125 mg) (considering the isolation of $[Pt_2(tpbz)(CH_3CN)_2(H_2O)_2](BF_4)_4$). $^{1}H$ NMR (400 MHz, $CD_3CN$): δ = 7.94 (tt, $J(^{1}H\text{-}^{31}P)$ = 69.7 Hz; $J(^{1}H\text{-}^{31}P)$ = 8.9 Hz, 2H, H-tpbz), 7.70-7.30 (m, 40H, Ph). $^{31}P\{^{1}H\}$ NMR (161.9 MHz, $CD_3CN$): δ = 40.0 (m(AA'XX'), $P_{trans\text{-}N}$, $^{2}J(^{31}P\text{-}^{195}Pt)$ = 3385 Hz, 33.7 (m(AA'XX'), $P_{trans\text{-}O}$ $^{2}J(^{31}P\text{-}^{195}Pt)$ = 3810 Hz). $^{19}F$ NMR (376 MHz, $CD_3CN$): δ = -154.7 (s, $^{10}BF_4$), -155.1 (s, $^{11}BF_4$). IR (KBr disk): $\tilde{\nu}$ = 2327, 2300, 1482, 1437, 1084, 1063, 996. ESI(+) Orbitrap *m/z*: 454.36 [**2Pt**-2$H_2O$+$CH_3CN$+Cl-4$BF_4$]$^{3+}$; calcd: 454.40; 342.03 [**2Pt**-2$H_2O$+2$CH_3CN$-4$BF_4$]$^{4+}$; calcd: 342.06; 331.78 [**2Pt**-2$H_2O$+$CH_3CN$-4$BF_4$]$^{4+}$; calcd: 331.81.

Synthesis of $[Pt_2(tpbz)(solvent)_4](PF_6)_4$ (**3Pt**)

From 105 mg (0.41 mmol) of $AgPF_6$ and 135 mg (0.10 mmol) of $[Pt_2Cl_4(tpbz)]$ compound **3Pt** was obtained as white solid in 74% yield (140 mg) (considering the isolation of $[Pt_2(tpbz)(CH_3CN)_2(H_2O)_2](PF_6)_4$. $^{1}H$ NMR (400 MHz, $CD_3CN$): δ = 7.94 (tt,

$J(^1H\text{-}^{31}P)$ = 65.6 Hz; $J(^1H\text{-}^{31}P)$ = 8.5 Hz, 2H, H-tpbz), 7.72-7.11 (m, 40H, Ph). $^{31}P\{^1H\}$ NMR (161.9 MHz, $CD_3CN$): δ = 40.0 (m(AA'XX'), $P_{trans\text{-}N}$, $^2J(^{31}P\text{-}^{195}Pt)$ = 3392 Hz, 33.7 (m(AA'XX'), $P_{trans\text{-}O}$ $^2J(^{31}P\text{-}^{195}Pt)$ = 3811 Hz), -144.6 (sept, $J(^{31}P\text{-}^{19}F)$ = 706 Hz, $PF_6$). $^{19}F$ NMR (376 MHz, $CD_3CN$): δ = -72.97 (d, $J(^{31}P\text{-}^{19}F)$ = 706 Hz, $PF_6$). IR (KBr disk): $\tilde{\nu}$ = 2333, 2305, 1483, 1439, 1104, 836.

Synthesis of $[Pt_2(tpbz)(solvent)_4](SbF_6)_4$ (**4Pt**)

From 140 mg (0.41 mmol) of $AgPF_6$ and 135 mg (0.10 mmol) of $[Pt_2Cl_4(tpbz)]$ compound **4Pt** was obtained as white solid in 66% yield (150 mg) (considering the isolation of $[Pt_2(tpbz)(CH_3CN)_2(H_2O)_2](SbF_6)_4$. $^1H$ NMR (400 MHz, $CD_3CN$): δ = 7.94 (tt, $J(^1H\text{-}^{31}P)$ = 66.0 Hz; $J(^1H\text{-}^{31}P)$ = 8.8 Hz, 2H, H-tpbz), 7.72-7.24 (m, 40H, Ph). $^{31}P\{^1H\}$ NMR (161.9 MHz, $CD_3CN$): δ = 40.0 (m(AA'XX'), $P_{trans\text{-}N}$, $^2J(^{31}P\text{-}^{195}Pt)$ = 3386 Hz, 33.7 (m(AA'XX'), $P_{trans\text{-}O}$ $^2J(^{31}P\text{-}^{195}Pt)$ = 3809 Hz). $^{19}F$ NMR (376 MHz, $CD_3CN$): δ = -124.0 (six, $J(^{121}Sb\text{-}^{19}F)$ = 1932 Hz; oct, $J(^{123}Sb\text{-}^{19}F)$ = 1045 Hz, $SbF_6$) IR (KBr disk): $\tilde{\nu}$ = 2337, 2310, 1483, 1439, 1104, 656. ESI(+) LC/MSD-TOF (acetone) *m/z*: 311.29 [**4Pt**-$2H_2O$-$CH_3CN$-$4SbF_6$]$^{4+}$; calcd: 311.29; 301.04 [**4Pt**-$2H_2O$-$CH_3CN$-$4SbF_6$]$^{4+}$; calcd: 301.04. ESI(+) Orbitrap (acetonitrile) *m/z*: 678.51 [**4Pt**-$2H_2O$+2Cl-$4SbF_6$]$^{2+}$; calcd: 678.57; 454.36 [**4Pt**-$2H_2O$+$CH_3CN$+Cl-$4SbF_6$]$^{3+}$; calcd: 454.40.

Synthesis of $[Pt_2(tpbz)(PF_2O_2)_4]$(**5Pt**)

Solid $AgPF_2O_2$ (85 mg, 0.41 mmol) was added to a dichloromethane/acetonitrile (20:20ml) suspension of $[Pt_2Cl_4(tpbz)]$ (135 mg, 0.10 mmol) at room temperature. After stirring in the dark overnight, the reaction mixture was filtered and the resulting solution evaporated to dryness. The solid residue was extracted with nitromethane (2x10 mL). The combined extracts were concentrated and after the addition of diethyl ether a white solid was obtained in 59% yield (95 mg). $^1H$ NMR (400 MHz, $CD_3NO_2$): δ = 8.16 (s br, 2H, H-tpbz), 7.75-7.21 (m, 40H, Ph). $^{31}P\{^1H\}$ NMR (161.9 MHz, $CD_3NO_2$): δ = 30.6 (s, $^2J(^{31}P\text{-}^{195}Pt)$ = 4099 Hz, tpbz), -15.9 (t, $^1J(^{31}P\text{-}^{19}F)$ = 768 Hz, $PF_2O_2^-$). $^{19}F$ NMR (376 MHz, $CD_3NO_2$): δ = - 81.3 (d, $^1J(^{31}P\text{-}^{19}F)$ = 968 Hz). IR (KBr disk): $\tilde{\nu}$ = 1483, 1437, 1297, 1131, 1102, 843.

Synthesis of $[\{Pd(\eta^3\text{-}2\text{-}Me\text{-}C_3H_4)\}_6(4\text{-}PPh_2py)_{12}\{Pd_2(tpbz)\}_3](CF_3SO_3)_{18}$ (**$1a_6$1$Pd_3$**)

Method A: To a dichloromethane solution (20 ml) of $[Pd(\eta^3\text{-}2\text{-}Me\text{-}C_3H_4)(COD)]$ $CF_3SO_3$ (25 mg, 0.06 mmol) were added successively 32 mg (0.12 mmol) of 4-$PPh_2$py and 53 mg (0.03 mmol) $[Pd_2(CH_3CN)_4(tpbz)](CF_3SO_3)_4$ as a solids at room temperature. After 2h of

stirring, the reaction mixture was filtered, concentrated to 5 ml under vacuum and precipitated with diethyl ether. A pale yellow solid was obtained in 76% yield (75 mg).

Method B: To a dichloromethane solution (20 ml) of the previously synthesized [Pd($\eta^3$-2-Me-$C_3H_4$)(4-$PPh_2py$)$_2$]$CF_3SO_3$ (**1a**) (50 mg, 0.06 mmol) solid [$Pd_2(CH_3CN)_4$(tpbz)]$(CF_3SO_3)_4$ (53 mg, 0.03 mmol) was added. After 2h of stirring, the reaction mixture was filtered, concentrated to 5 ml under vacuum and precipitated with diethyl ether. A pale yellow solid was obtained in 86% yield (85 mg). $^1$H NMR (400 MHz, $CD_2Cl_2$): δ = 8.88 (s br, 24H, $H_{\alpha\text{-py}}$), 8.05-6.84 (m, 270H, Ph+$H_{\beta\text{-py}}$), 3.51 (s, 12$H_{syn}$, Me-$C_3H_4$), 2.27 (s br, 12$H_{anti}$, Me-$C_3H_4$), 1.87 (s, 18H, *Me*-$C_3H_4$). $^{31}$P{$^1$H} NMR (161.9 MHz, $CD_2Cl_2$): δ = 55.2 (s, tpbz), 25.6 (s, $PPh_2py$). $^{19}$F NMR (376 MHz, $CD_2Cl_2$): δ = -78.6. IR (KBr disk): $\tilde{\nu}$ = 1601, 1485, 1440, 1277, 1164, 1029. ESI(+) Q/TOF *m/z*: 2324.55 [**1a$_6$1Pd$_3$**-4$CF_3SO_3$]$^{4+}$; calcd: 2324.56; 2115.18 [**1a$_6$1Pd$_3$-1a**-4$CF_3SO_3$]$^{4+}$; calcd: 2115.29; 1830.80 [**1a$_6$1Pd$_3$**-5$CF_3SO_3$]$^{5+}$; calcd: 1829.85; 1662.21 [**1a$_6$1Pd$_3$-1a**-5$CF_3SO_3$]$^{5+}$; calcd: 1662.24; 1499.88 [**1a$_6$1Pd$_3$**-6$CF_3SO_3$]$^{6+}$; calcd: 1499.89; 687.16 [**1a**-$CF_3SO_3$]$^+$; calcd: 687.19.

Metallamacrocycles **na$_6$nPd$_3$** and **na$_6$nPt$_3$** were synthesized following analogous procedures to those described for compound **1a$_6$1Pd$_3$**.

Synthesis of [{Pd($\eta^3$-2-Me-$C_3H_4$)}$_6$(4-$PPh_2py$)$_{12}$\{$Pt_2$(tpbz)\}$_3$]$(CF_3SO_3)_{18}$ (**1a$_6$1Pt$_3$**)

Method A. From 25 mg (0.06 mmol) of [Pd($\eta^3$-2-Me-$C_3H_4$)(COD)]$CF_3SO_3$, 32 mg (0.12 mmol) of 4-$PPh_2py$ and 60 mg (0.03 mmol) of [$Pt_2(CH_3CN)_2(H_2O)_2$(tpbz)]$(CF_3SO_3)_4$ compound (**1a$_6$1Pt$_3$**) was obtained as a white solid in 77% yield (80 mg).

Method B: From 50 mg (0.06 mmol) of [Pd($\eta^3$-2-Me-$C_3H_4$)(4-$PPh_2py$)$_2$]$CF_3SO_3$ (**1a**) and 60 mg (0.03 mmol) of [$Pt_2(CH_3CN)_2(H_2O)_2$(tpbz)]$(CF_3SO_3)_4$ compound (**1a$_6$1Pt$_3$**) was obtained as a white solid in 86% yield (90 mg). $^1$H NMR (400 MHz, $CD_2Cl_2$): δ = 8.89 (s br, 24H, $H_{\alpha\text{-py}}$), 8.13-6.14 (m, 270H, Ph+$H_{\beta\text{-py}}$), 3.62 (s, 12$H_{syn}$, Me-$C_3H_4$), 2.25 (m, 12$H_{anti}$, Me-$C_3H_4$), 1.90 (s, 18H, *Me*-$C_3H_4$). $^{31}$P{$^1$H} NMR (161.9 MHz, $CD_2Cl_2$): δ = 29.1 (s, $^2J$($^{31}$P-$^{195}$Pt) = 3245 Hz, tpbz), 26.0 (s, $PPh_2py$). $^{19}$F NMR (376 MHz, $CD_2Cl_2$): δ = -78.1. IR (KBr disk): $\tilde{\nu}$ = 1595, 1485, 1440, 1277, 1166, 1030. ESI(+) Orbitrap *m/z*: 1936.1164 [**1a$_6$1Pt$_3$**-5$CF_3SO_3$]$^{5+}$; calcd: 1936.1267; 1588.6135 [**1a$_6$1Pt$_3$**-6$CF_3SO_3$]$^{6+}$; calcd: 1936.6135; 1340.3662 [**1a$_6$1Pt$_3$**-7$CF_3SO_3$]$^{7+}$; calcd: 1340.3898; 687.1317 [**1a**-$CF_3SO_3$]$^+$; calcd: 687.1319.

Synthesis of [{Pd($\eta^3$-2-Me-$C_3H_4$)}$_6$(4-$PPh_2py$)$_{12}$\{$Pd_2$(tpbz)\}$_3$]$(BF_4)_{18}$ (**2a$_6$2Pd$_3$**)

Method A. From 22 mg (0.06 mmol) of $[Pd(\eta^3\text{-}2\text{-}Me\text{-}C_3H_4)(COD)]BF_4$, 32 mg (0.12 mmol) of 4-$PPh_2py$ and 45 mg (0.03 mmol) of $[Pd_2(tpbz)(CH_3CN)_4](BF_4)_4$ (**2Pd**) compound $\mathbf{2a_6 2Pd_3}$ was obtained as a white solid in 80% yield (70 mg).

Method B: From 45 mg (0.06 mmol) of $[Pd(\eta^3\text{-}2\text{-}Me\text{-}C_3H_4)(4\text{-}PPh_2py)_2]BF_4$ (**2a**) and 45 mg (0.03 mmol) of $[Pd_2(tpbz)(CH_3CN)_4](BF_4)_4$ (**2Pd**) compound $\mathbf{2a_6 2Pt_3}$ was obtained as a white solid in 91% yield (80 mg). $^1$H NMR (400 MHz, $CD_2Cl_2$): δ = 8.69 (s br, 24H, $H_{\alpha\text{-}py}$), 8.10-6.77 (m, 270H, Ph+$H_{\beta\text{-}py}$), 3.66 (s, 12$H_{syn}$, Me-$C_3H_4$), 2.13 (m, 12$H_{anti}$, Me-$C_3H_4$), 1.91 (s, 18H, *Me*-$C_3H_4$). $^{31}P\{^1H\}$ NMR (161.9 MHz, $CD_2Cl_2$): δ = 57.6 (s, tpbz), 25.0 (s, $PPh_2py$). $^{19}$F NMR (376 MHz, $CD_2Cl_2$): δ = -146.7 (s br, $BF_4^-)_{in}$, -150.7 (s, $BF_4)_{out}$. IR (KBr disk): $\tilde{\nu}$ = 1597 , 1481, 1442, 1100, 1084, 1060, 995. ESI(+) Q/TOF *m/z*: 2106.4661 [$\mathbf{2a_6 2Pd_3}$-4$BF_4$]$^{4+}$; calcd: 2106.4874; 1667.7846 [$\mathbf{2a_6 2Pd_3}$-5$BF_4$]$^{5+}$; calcd: 1667.7891; 1375.4906 [$\mathbf{2a_6 2Pd_3}$-6$BF_4$]$^{6+}$; calcd: 1375.4902; 1166.5715 [$\mathbf{2a_6 2Pd_3}$-7$BF_4$]$^{7+}$; calcd: 1166.5624; 687.1283 [**2a**-$BF_4$]$^+$; calcd: 687.1319.

Synthesis of $[\{Pd(\eta^3\text{-}2\text{-}Me\text{-}C_3H_4)\}_6(4\text{-}PPh_2py)_{12}\{Pt_2(tpbz)\}_3](BF_4)_{18}$ ($\mathbf{2a_6 2Pt_3}$)

Method A. From 22 mg (0.06 mmol) of $[Pd(\eta^3\text{-}2\text{-}Me\text{-}C_3H_4)(COD)]BF_4$, 32 mg (0.12 mmol) of 4-$PPh_2py$ and 50 mg (0.03 mmol) of $[Pt_2(tpbz)(CH_3CN)_2(H_2O)_2](BF_4)_4$ (**2Pt**) compound $\mathbf{2a_6 2Pt_3}$ was obtained as a white solid in 81% yield (75 mg).

Method B: From 45 mg (0.06 mmol) of $[Pd(\eta^3\text{-}2\text{-}Me\text{-}C_3H_4)(4\text{-}PPh_2py)_2]BF_4$ (**2a**) and 50 mg (0.03 mmol) of $[Pt_2(tpbz)(CH_3CN)_2(H_2O)_2](BF_4)_4$ (**2Pt**) compound $\mathbf{2a_6 2Pt_3}$ was obtained as a white solid in 86% yield (80 mg). $^1$H NMR (400 MHz, $CD_2Cl_2$): δ = 8.69 (s br, 24H, $H_{\alpha\text{-}py}$), 8.14-6.79 (m, 270H, Ph+$H_{\beta\text{-}py}$), 3.75 (s, 12$H_{syn}$, Me-$C_3H_4$), 2.10 (m, 12$H_{anti}$, Me-$C_3H_4$), 1.92 (s, 18H, *Me*-$C_3H_4$). $^{31}P\{^1H\}$ NMR (161.9 MHz, $CD_2Cl_2$): δ = 30.6 (s, $^2J(^{31}P\text{-}^{195}Pt)$ = 3270 Hz, tpbz), 25.9 (s, $PPh_2py$). δ = 57.6 (s, tpbz), 25.0 (s, $PPh_2py$). $^{19}$F NMR (376 MHz, $CD_2Cl_2$): δ = -146.6 (s br, $BF_4^-)_{in}$, -151.0 (s, $BF_4)_{out}$. IR (KBr disk): $\tilde{\nu}$ = 1601 , 1481, 1437, 1099, 1057, 996. ESI(+)Q/TOF *m/z*: 1464.0421 [$\mathbf{2a_6 2Pt_3}$-6$BF_4$]$^{6+}$; calcd: 1464.0503; 1242.4517 [$\mathbf{2a_6 2Pt_3}$-7$BF_4$]$^{7+}$; calcd: 1242.4710; 1076.3908 [$\mathbf{2a_6 2Pt_3}$-8$BF_4$]$^{8+}$; calcd: 1076.4117; 687.1220 [**2a**-$BF_4$]$^+$; calcd: 687.1319. LC/MSD-TOF *m/z*: 3014.95 [$\mathbf{2a_6 2Pt_3}$-3$BF_4$]$^{3+}$; calcd: 3015.10; 2239.66 [$\mathbf{2a_6 2Pt_3}$-4$BF_4$]$^{4+}$; calcd: 2239.58; 1774.41 [$\mathbf{2a_6 2Pt_3}$-5$BF_4$]$^{5+}$; calcd: 1774.26; 1464.18 [$\mathbf{2a_6 2Pt_3}$-6$BF_4$]$^{6+}$; calcd: 1464.05; 1242.59 [$\mathbf{2a_6 2Pt_3}$-7$BF_4$]$^{7+}$; calcd: 1242.47.

Synthesis of $[\{Pd(\eta^3\text{-}2\text{-}Me\text{-}C_3H_4)\}_6(4\text{-}PPh_2py)_{12}\{Pd_2(tpbz)\}_3](PF_6)_{18}$ ($\mathbf{3a_6 3Pd_3}$)

Method A. From 25 mg (0.06 mmol) of $[Pd(\eta^3\text{-}2\text{-}Me\text{-}C_3H_4)(COD)]PF_6$, 32 mg (0.12 mmol) of 4-$PPh_2py$ and 55 mg (0.03 mmol) of $[Pd_2(tpbz)(CH_3CN)_4](BF_4)_4$ (**3Pd**) compound $\mathbf{3a_6 3Pd_3}$ was obtained as a white solid in 81% yield (80 mg).

Method B: From 50 mg (0.06 mmol) of $[Pd(\eta^3\text{-}2\text{-}Me\text{-}C_3H_4)(4\text{-}PPh_2py)_2]PF_6$ (**3a**) and 55 mg (0.03 mmol) of $[Pd_2(tpbz)(CH_3CN)_4](PF_6)_4$ (**3Pd**) compound $\mathbf{3a_6 3Pd_3}$ was obtained as a white solid in 92% yield (90 mg). $^1$H NMR (400 MHz, $CD_2Cl_2$): δ = 8.58 (s br, 24H, $H_{\alpha\text{-}py}$), 8.00-6.75 (m, 270H, Ph+$H_{\beta\text{-}py}$), 3.74 (s, 12$H_{syn}$, Me-$C_3H_4$), 1.99 (m, 12$H_{anti}$, Me-$C_3H_4$), 1.88 (s, 18H, *Me*-$C_3H_4$). $^{31}$P{$^1$H} NMR (161.9 MHz, $CD_2Cl_2$): δ = 56.6 (s, tpbz), 25.6 (s, $PPh_2py$), -144.3 (sept, $J(^{31}P\text{-}^{19}F)$ = 713 Hz, $PF_6^-$). $^{19}$F NMR (376 MHz, $CD_2Cl_2$): δ = -68.2 (d, $J(^{31}P\text{-}^{19}F)$= 714 Hz, $PF_6)_{in}$, -71.8 (d, $J(^{31}P\text{-}^{19}F)$ = 714 Hz, $PF_6)_{out}$. IR (KBr disk): $\tilde{\nu}$ = 1575, 1481, 1437, 1100, 840. ESI(+) Q/TOF *m/z*: 1491.64 $[\mathbf{3a_6 3Pd_3}\text{-}6PF_6]^{6+}$; calcd: 1491.74; 1257.87 $[\mathbf{3a_6 3Pt_3}\text{-}7PF_6]^{7+}$; calcd: 1257.93.

Synthesis of $[\{Pd(\eta^3\text{-}2\text{-}Me\text{-}C_3H_4)\}_6(4\text{-}PPh_2py)_{12}\{Pt_2(tpbz)\}_3](PF_6)_6(PF_2O_2)_{12}$ ($\mathbf{3a_6 5Pt_3}$)

Method A. From 25 mg (0.06 mmol) of $[Pd(\eta^3\text{-}2\text{-}Me\text{-}C_3H_4)(COD)]PF_6$, 32 mg (0.12 mmol) of 4-$PPh_2py$ and 50 mg (0.03 mmol) of $[Pt_2(tpbz)(PF_2O_2)_4]$ (**5Pt**) compound $\mathbf{3a_6 5Pt_3}$ was obtained as a white solid in 71% yield (70 mg).

Method B: From 50 mg (0.06 mmol) of $[Pd(\eta^3\text{-}2\text{-}Me\text{-}C_3H_4)(4\text{-}PPh_2py)_2]PF_6$ (**3a**) and 50 mg (0.03 mmol) of $[Pt_2(tpbz)(PF_2O_2)_4]$ (**5Pt**) compound $\mathbf{3a_6 5Pt_3}$ was obtained as a white solid in 76% yield (75 mg). $^1$H NMR (400 MHz, $CD_2Cl_2$): δ = 8.95 (s br, 24H, $H_{\alpha\text{-}py}$), 8.10-6.78 (m, 270H, Ph+$H_{\beta\text{-}py}$), 3.77 (s br, 12$H_{syn}$, Me-$C_3H_4$), 1.90 (s br, 30H, Me-$C_3H_2H_{anti}$+*Me*-$C_3H_4$). $^{31}$P{$^1$H} NMR (161.9 MHz, $CD_2Cl_2$): δ = 30.0 (s, $^2J(^{31}P\text{-}^{195}Pt)$ = 3248 Hz, tpbz), 25.8 (s, $PPh_2py$), 14.4 (t, $^2J(^{31}P\text{-}^{19}F)$ = 962 Hz, $PF_2O_2^-$), -144.4 (sept, $^2J(^{31}P\text{-}^{19}F)$ = 712 Hz, $PF_6^-$). $^{19}$F NMR (376 MHz, $CD_2Cl_2$): ): δ = -68.5 (d, $J(^{31}P\text{-}^{19}F)$= 713 Hz, $PF_6^-)_{in}$, -73.0 (d, $J(^{31}P\text{-}^{19}F)$= 713 Hz, $PF_6^-)_{out}$, -81.2 (d, $J(^{31}P\text{-}^{19}F)$= 962 Hz, $PF_2O_2^-$). IR (KBr disk): $\tilde{\nu}$ = 1602 , 1482, 1437, 1299, 1100, 839.

Synthesis of $[\{Pd(\eta^3\text{-}2\text{-}Me\text{-}C_3H_4)\}_6(4\text{-}PPh_2py)_{12}\{Pd_2(tpbz)\}_3](SbF_6)_{18}$ ($\mathbf{4a_6 4Pd_3}$)

Method A. From 30 mg (0.06 mmol) of $[Pd(\eta^3\text{-}2\text{-}Me\text{-}C_3H_4)(COD)]SbF_6$, 32 mg (0.12 mmol) of 4-$PPh_2py$ and 60 mg (0.03 mmol) of $[Pd_2(tpbz)(H_2O)_4](SbF_6)_4$ (**4Pd**) compound $\mathbf{4a_6 4Pd_3}$ was obtained as a white solid in 57% yield (65 mg).

Method B: From 55 mg (0.06 mmol) of $[Pd(\eta^3\text{-}2\text{-}Me\text{-}C_3H_4)(4\text{-}PPh_2py)_2]SbF_6$ (**4a**) and 60 mg (0.03 mmol) of $[Pd_2(tpbz)(H_2O)_4](SbF_6)_4$ (**4Pd**) compound $\mathbf{4a_6 4Pt_3}$ was obtained as a white solid in 61% yield (70 mg). $^1$H NMR (400 MHz, $CD_2Cl_2$): δ = 8.56 (s br, 24H,

$H_{\alpha\text{-py}}$), 8.06-6.76 (m, 270H, Ph+$H_{\beta\text{-py}}$), 3.77 (s, 12$H_{syn}$, Me-$C_3H_4$), 2.01 (m, 12$H_{anti}$, Me-$C_3H_4$), 1.89 (s, 18H, *Me*-$C_3H_4$). $^{31}P\{^1H\}$ NMR (161.9 MHz, $CD_2Cl_2$): δ = 56.4 (s, tpbz), 25.6 (s, $PPh_2py$). IR (KBr disk): $\tilde{\nu}$ = 1597, 1481, 1438, 1199, 692, 658.

Synthesis of $[\{Pd(\eta^3\text{-2-Me-}C_3H_4)\}_6(4\text{-}PPh_2py)_{12}\{Pt_2(tpbz)\}_3](SbF_6)_{18}$ (**4a$_6$4Pt$_3$**)

Method A. From 30 mg (0.06 mmol) of $[Pd(\eta^3\text{-2-Me-}C_3H_4)(COD)]SbF_6$, 32 mg (0.12 mmol) of 4-$PPh_2py$ and 70 mg (0.03 mmol) of $[Pt_2(tpbz)(CH_3CN)_2(H_2O)_2](SbF_6)_4$ (**4Pt**) compound **4a$_6$4Pt$_3$** was obtained as a white solid in 75% yield (90 mg).

Method B: From 55 mg (0.06 mmol) of $[Pd(\eta^3\text{-2-Me-}C_3H_4)(4\text{-}PPh_2py)_2]SbF_6$ (**4a**) and 70 mg (0.03 mmol) of $[Pt_2(tpbz)(CH_3CN)_2(H_2O)_2](SbF_6)_4$ (**4Pt**) compound **4a$_6$4Pt$_3$** was obtained as a white solid in 83% yield (100 mg). $^1H$ NMR (400 MHz, $CD_2Cl_2$): δ = 9.00-8.40 ( br, 24H, $H_{\alpha\text{-py}}$), 8.12-6.75 (m, 270H, Ph+$H_{\beta\text{-py}}$), 3.84 (s br, 12$H_{syn}$, Me-$C_3H_4$), 2.01 (m, 12$H_{anti}$, Me-$C_3H_4$), 1.90 (s, 18H, *Me*-$C_3H_4$). $^{31}P\{^1H\}$ NMR (161.9 MHz, $CD_2Cl_2$): δ = 29.5 (s, $^2J(^{31}P\text{-}^{195}Pt)$ = 3240 Hz, tpbz), 25.9 (s, $PPh_2py$). IR (KBr disk): $\tilde{\nu}$ = 1602 , 1482, 1438, 1100, 839, 693, 660. ESI(+) LC/MSD-TOF *m/z*: 2760.92 [**4a$_6$4Pt$_3$**-4$SbF_6$]$^{4+}$; calcd: 2760.95; 2161.53 [**4a$_6$4Pt$_3$**-5$SbF_6$]$^{5+}$; calcd: 2161.58; 1761.83 [**4a$_6$4Pt$_3$**-6$SbF_6$]$^{6+}$; calcd: 1762.00; 1476.44 [**4a$_6$4Pt$_3$**-7$SbF_6$]$^{7+}$; calcd: 1476.59; 1262.39 [**4a$_6$4Pt$_3$**-8$SbF_6$]$^{8+}$; calcd: 1262.53.


## Acknowledgements

Financial support for this work was provided by Ministerio de Economía y Competitividad (MINECO/FEDER) of Spain (Projects CTQ2015-65040 and CTQ2015-65707-C2-1-P, PGC2018-093863-B-C21 and MDM-2017-0767). E.R. thanks Generalitat de Catalunya for an ICREA Academia award and for the SGR2017-1289 grant. The authors acknowledge the general facilities of the University of Barcelona (CCiT-UB) and the computer resources, technical expertise and assistance provided by the Consorci de Serveis Universitaris de Catalunya.


## References


[1] a) S. Leininger, B. Olenyuk and P. J. Stang, *Chem. Rev.*, 2000, **100**, 853-907; b) S. R. Seidel and P. J. Stang, *Acc. Chem. Res.*, 2002, **35**, 972-983; c) L. Cronin, *Annu. Rep. Prog. Chem., Sect. A, Inorg. Chem.*, 2004, **100**, 323-383; d) C. H. M. Amijs, G. P. M. van Klink and G. van Koten, *Dalton Trans.*, 2006, 308-327; e) J. R. Nitschke, *Acc. Chem. Res.*, 2007, **40**, 103-112; f) K. Ariga, J. P. Hill, M. V. Lee, A. Vinu, R. Charvet and S. Acharya, *Sci. Technol. Adv. Mater.*, 2008, **9**, 1-97; g) R. Chakrabarty, P. S. Mukherjee and P. J. Stang, *Chem. Rev.*, 2011, **111**,

6810-6918; h) S. Mukherjee and P. S. Mukherjee, *Chem. Commun.*, 2014, **50**, 2239-2248; i) T. R. Cook and P. J. Stang, *Chem. Rev.*, 2015, **115**, 7001-7045; j) B. Li, T. He, Y. Fan, X. Yuan, H. Qiu and S. Yin, *Chem. Commun.*, 2019, **55**, 8036-8059; k) D. Zhang, T. K. Ronson and J. R. Nitschke, *Acc. Chem. Res.*, 2018, **51**, 2423-2436; l) Y. Sun, C. Chen and P. J. Stang, *Acc. Chem. Res.*, 2019, **52**, 802-817.

[2] a) A. Kumar, S. S. Sun and A. J. Lees, *Coord. Chem. Rev.*, 2008, **252**, 922-939; b) X. Zhang, T. Chen, H. J. Yan, D. Wang, Q. H. Fan, L. J. Wan, K. Ghosh, H. B. Yang and P. J. Stang, *Acs Nano*, 2010, **4**, 5685-5692; c) P. D. Frischmann and M. J. MacLachlan, *Chem. Soc. Rev.*, 2013, **42**, 871-890.

[3] a) M. W. Cooke, D. Chartrand and G. S. Hanan, *Coord. Chem. Rev.*, 2008, **252**, 903-921; b) R. Saha and P. S. Mukherjee, *Dalton Trans.*, 2020, **49**, 1716-1720.

[4] V. Croue, S. Goeb and M. Salle, *Chem. Commun.*, 2015, **51**, 7275-7289.

[5] a) D. Fiedler, D. H. Leung, R. G. Bergman and K. N. Raymond, *Acc. Chem. Res.*, 2005, **38**, 349-358; b) J. Lee, O. K. Farha, J. Roberts, K. A. Scheidt, S. T. Nguyen and J. T. Hupp, *Chem. Soc. Rev.*, 2009, **38**, 1450-1459; c) L. Chen, H. Yang and M. Shionoya, *Chem. Soc. Rev.*, 2017, **46**, 2555-2576; d) I. Sinha and P. S. Mukherjee, *Inorg. Chem.*, 2018, **57**, 4205-4221.

[6] H. Sepehrpour, W. Fu, Y. Sun and P. J. Stang, *J. Am. Chem. Soc.*, 2019, **141**, 14005-14020.

[7] a) N. Gimeno and R. Vilar, *Coord. Chem. Rev.*, 2006, **250**, 3161-3189; b) R. Vilar, *Eur. J. Inorg. Chem.*, 2008, 357-367; c) R. Custelcean, *Chem. Soc. Rev.*, 2014, **43**, 1813-1824; d) H. T. Chifotides and K. R. Dunbar, *Acc. Chem. Res.*, 2013, **46**, 894-906.

[8] D. Semeril, D. Matt, J. Harrowfield, N. Schultheiss and L. Toupet, *Dalton Trans.*, 2009, 6296-6298.

[9] a) I. Angurell, M. Ferrer, A. Gutiérrez, M. Martínez, M. Rocamora, L. Rodríguez, O. Rossell, Y. Lorenz and M. Engeser, *Chem.-Eur. J.*, 2014, **20**, 14473-14487; b) Y. Lorenz, A. Gutiérrez, M. Ferrer and M. Engeser, *Inorg. Chem.*, 2018, **57**, 7346-7354.

[10] a) H. Tsuji, *Palladium Reagents and Catalysis*, Wiley, Chichester, UK, 2004; b) T. V. RajanBabu, *Chem. Rev.*, 2003, **103**, 2845-2860; c) L. Milhan and P. J. Guiry, in *Transition Metal Catalysed Enantioselective allylic Substitution in Organic Synthesis*, ed. U. Kazmaier, Springer-Verlag, Heidelberg, 2012.

[11] S. L. James, *Chem. Soc. Rev.*, 2009, **38**, 1744-1758.

[12] a) P. M. VanCalcar, M. M. Olmstead and A. L. Balch, *Chem. Commun.*, 1996, 2597-2598; b) E. Menozzi, M. Busi, C. Massera, F. Ugozzoli, D. Zuccaccia, A. Macchioni and E. Dalcanale, *J. Org. Chem.*, 2006, **71**, 2617-2624; c) E. Menozzi, M. Busi, R. Ramingo, M. Campagnolo, S. Geremia and E. Dalcanale, *Chem.-Eur. J.*, 2005, **11**, 3136-3148; d) S. H. Lim, Y. X. Su and S. M. Cohen, *Angew. Chem. Int. Ed.*, 2012, **51**, 5106-5109.

[13] J. Y. Zhang, P. W. Miller, M. Nieuwenhuyzen and S. L. James, *Chem.-Eur. J.*, 2006, **12**, 2448-2453.

[14] I. Angurell, M. Ferrer, A. Gutierrez, M. Martinez, L. Rodriguez, O. Rossell and M. Engeser, *Chem.-Eur. J.*, 2010, **16**, 13960-13964.

[15] a) B. R. Manzano, F. A. Jalón, M. L. Soriano, M. C. Carrión, M. P. Carranza, K. Mereiter, A. M. Rodríguez, A. de la Hoz and A. Sánchez-Migallón, *Inorg. Chem.*, 2008, **47**, 8957-8971; b) G. Dura, M. Carrion, F. Jalón, A. Rodriguez and B. Manzano, *Cryst. Growth Des.*, 2014, **14**, 3510-3529.

[16] a) H. T. Chifotides, I. D. Giles and K. R. Dunbar, *J. Am. Chem. Soc.*, 2013, **135**, 3039-3055; b) R. Sekiya, M. Fukuda and R. Kuroda, *J. Am. Chem. Soc.*, 2012, **134**, 10987-10997.
[17] M. O. Awaleh, A. Badia and F. Brisse, *Cryst. Growth Des.*, 2005, **5**, 1897-1906.
[18] Y. Yamashina, Y. Kataoka and Y. Ura, *Eur. J. Inorg. Chem.*, 2014, 4073-4078.
[19] R. Díaz-Torres and S. Alvarez, *Dalton Trans.*, 2011, **40**, 10742-10750.
[20] The mass spectra of both $[\{Pd(\eta^3\text{-}2\text{-}Me\text{-}C_3H_4)\}_6(4\text{-}PPh_2py)_{12}\{Pt_2(tpbz)\}_3](PF_6)_6(PF_2O_2)_{12}$ ($3a_65Pt_3$) and $[\{Pd(\eta^3\text{-}2\text{-}Me\text{-}C_3H_4)\}_6(4\text{-}PPh_2py)_{12}\{Pd_2(tpbz)\}_3](SbF_6)_{18}$ ($4a_64Pd_3$) species have been not included because they only showed a complicated mixture of fragments and no peaks corresponding to metallamacrocycles can be observed under ESI conditions.
[21] a) A. J. Blake, G. Baum, N. R. Champness, S. S. M. Chung, P. A. Cooke, D. Fenske, A. N. Khlobystov, D. A. Lemenovskii, W.-S. Li and M. Schröder, *J. Chem. Soc., Dalton Trans.*, 2000, 4285-4291; b) P. Ovejero, M. J. Mayoral, M. Cano, J. A. Campo, J. V. Heras, E. Pinilla and M. R. Torres, *J. Organomet. Chem.*, 2007, **692**, 4093-4105; c) S. M. Kim, J. H. Park and Y. K. Chung, *Chem. Commun.*, 2011, **47**, 6719-6721.
[22] A. Castilla, T. Ronson and J. Nitschke, *J. Am. Chem. Soc.*, 2016, **138**, 2342-2351.
[23] C. S. Campos-Fernández, B. L. Schottel, H. T. Chifotides, J. K. Bera, J. Bacsa, J. M. Koomen, D. H. Russell and K. R. Dunbar, *J. Am. Chem. Soc.*, 2005, **127**, 12909-12923.
[24] a) B. M. Trost and D. L. VanVranken, *Chem. Rev.*, 1996, **96**, 395-422; b) B. M. Trost and C. Lee, in *Catalytic Asymmetric Synthesis* ed. I. Ojima, Wiley-VCH, New York, 2000.
[25] T. Hayashi, M. Kawatsura and Y. Uozumi, *J. Am. Chem. Soc.*, 1998, **120**, 1681-1687.
[26] a) R. J. van Haaren, C. J. M. Druijven, G. P. F. van Strijdonck, H. Oevering, J. N. H. Reek, P. C. J. Kamer and P. W. N. M. van Leeuwen, *J. Chem. Soc., Dalton Trans.*, 2000, 1549-1554; b) M. D. K. Boele, P. C. J. Kamer, M. Lutz, A. L. Spek, J. G. de Vries, P. W. N. M. van Leeuwen and G. P. F. van Strijdonck, *Chem.-Eur. J.*, 2004, **10**, 6197-6197; c) S. C. Milheiro and J. W. Faller, *J. Organomet. Chem.*, 2011, **696**, 879-886.
[27] a) V. F. Slagt, M. Roder, P. C. J. Kamer, P. W. N. M. van Leeuwen and J. N. H. Reek, *J. Am. Chem. Soc.*, 2004, **126**, 4056-4057; b) V. F. Slagt, P. W. N. M. van Leeuwen and J. N. H. Reek, *Dalton Trans.*, 2007, 2302-2310; c) P. E. Goudriaan, X. B. Jang, M. Kuil, R. Lemmens, P. W. N. M. Van Leeuwen and J. N. H. Reek, *Eur. J. Org. Chem.*, 2008, 6079-6092.
[28] a) B. Olenyuk, J. A. Whiteford and P. J. Stang, *J. Am. Chem. Soc.*, 1996, **118**, 8221-8230; b) J. Fan, J. A. Whiteford, B. Olenyuk, M. D. Levin, P. J. Stang and E. B. Fleischer, *J. Am. Chem. Soc.*, 1999, **121**, 2741-2752.
[29] W. T. Dent, R. Long and A. J. Wilkinson, *J. Chem. Soc.*, 1964, 1585-1588.
[30] D. A. White, *Inorg. Synth.*, 1972, **13**, 55-62.
[31] a) G. R. Newkome and D. C. Hager, *J. Org. Chem.*, 1978, **43**, 947-949; b) L. Hirsivaara, M. Haukka and J. Pursiainen, *J. Organomet. Chem.*, 2001, **633**, 66-68.
[32] M. Ferrer, L. Giménez, A. Gutiérrez, J. C. Lima, M. Martínez, L. Rodríguez, A. Martín, R. Puttreddy and K. Rissanen, *Dalton Trans.*, 2017, **46**, 13920-13934.
[33] Z. Otwinowski and W. Minor, *Methods Enzymol.*, 1997, **276**, 307-326.
[34] A. L. J. Spek, *J. Appl. Cryst.*, 2003, **36**, 7-13.

[35] a) C. Bannwarth, S. Ehlert and S. Grimme, *J. Chem. Theory Comput.* , 2019, **15**, 1652-1671; b) M. Bursch, H. Neugebauer and S. Grimme, *Angew. Chem. Int. Ed.*, 2019, **58**, 11078-11087; c) S. Grimme, C. Bannwarth and P. Shushkov, *J. Chem. Theory Comput.*, 2017, **13**, 1989-2009.

[36] A. D. Becke, *J. Chem. Phys.*, 1993, **98**, 5648-5652.

[37] M. J. Frisch, G. W. Trucks, H. B. Schlegel, G. E. Scuseria, M. A. Robb, J. R. Cheeseman, G. Scalmani, V. Barone, B. Mennucci, G. A. Petersson, H. Nakatsuji, M. Caricato, X. Li, H. P. Hratchian, A. F. Izmaylov, J. Bloino, G. Zheng, J. L. Sonnenberg, M. E. Hada, M., K. Toyota, R. Fukuda, J. Hasegawa, M. Ishida, T. Nakajima, Y. Honda, O. Kitao, H. Nakai, T. Vreven, J. A. Montgomery, J. E. Peralta, F. Ogliaro, M. Bearpark, J. J. Heyd, E. Brothers, K. N. Kudin, V. N. Staroverov, R. Kobayashi, J. Normand, K. Raghavachari, A. Rendell, J. C. Burant, S. S. Iyengar, J. Tomasi, M. Cossi, N. Rega, N. J. Millam, M. Klene, J. E. Knox, J. B. Cross, V. Bakken, C. Adamo, J. Jaramillo, R. Gomperts, R. E. Stratmann, O. Yazyev, A. J. Austin, R. Cammi, C. Pomelli, J. W. Ochterski, R. L. Martin, K. Morokuma, V. G. Zakrzewski, G. A. Voth, P. Salvador, J. J. Dannenberg, S. Dapprich, A. D. Daniels, Ö. Farkas, J. B. Foresman, J. V. Ortiz, J. Cioslowski and D. J. Fox, *Gaussian 09 (Revision D.1)*, Wallingford, CT, 2009.

[38] a) V. Barone and M. Cossi, *J. Phys. Chem. A*, 1998, **102**, 1995-2001; b) M. R. Chierotti and R. Gobetto, *Chem. Commun.*, 2008, 1621-1634.

TOC

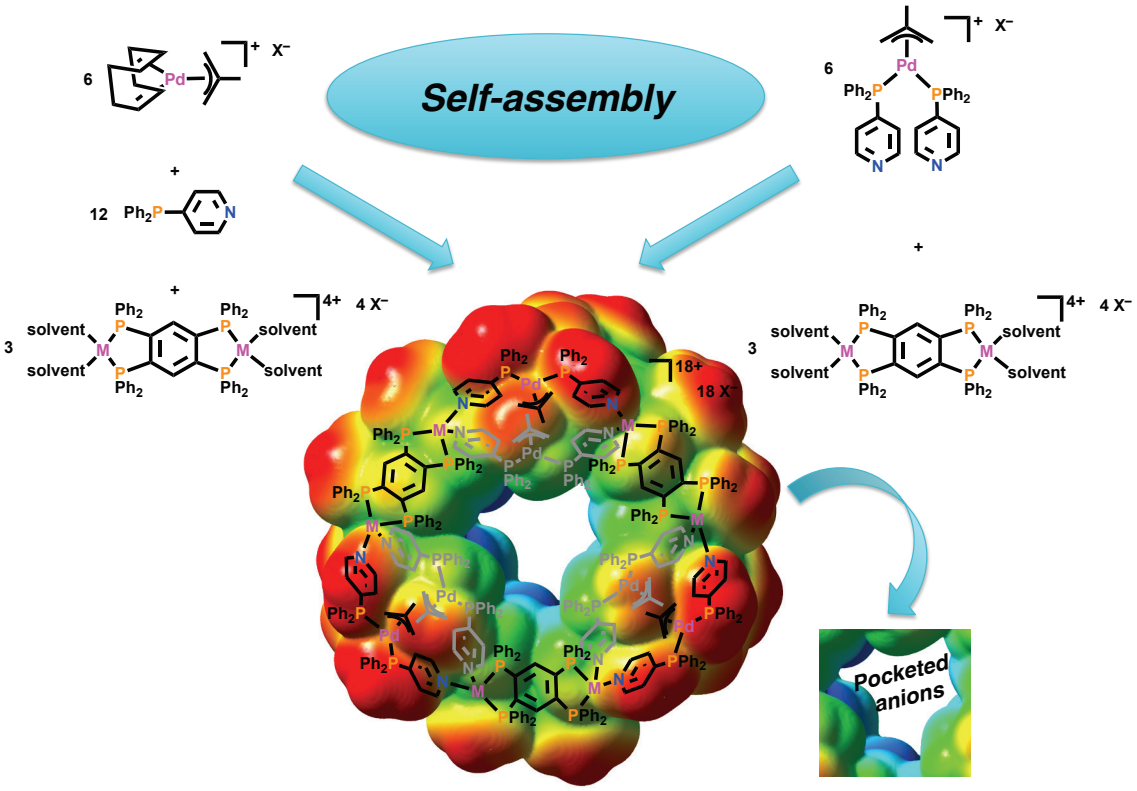


King-size positively charged void: selective self-assembly of crown-like high positive charge and 18-th nuclearity metallamacrocyles, study of their interaction with fluoroanions and catalytic activity.

Keywords: self-assembly, metallacycles, noncovalent interactions, allyl compounds, fluoroanions.